

A study on a novel continuous blood viscosity monitoring method for cardiopulmonary bypass

(人工心肺における新しい連続血液粘度モニタリング法に関する研究)

学位取得年月 2017 年 3 月

岡原 重幸

Contents

Chapter 1	Introduction.....	1
1.1	Background and purpose.....	1
1.2	Related works.....	3
1.3	Outline.....	4
Chapter 2	Hydrodynamic characteristics of a membrane oxygenator: modeling of pressure-flow characteristics and their influence on apparent viscosity	6
2.1	Introduction.....	6
2.2	Materials and methods	7
2.2.1	Experiments.....	7
2.2.2	Pressure gradient characteristics approximation equation ...	11
2.2.3	Simulations with approximation equation.....	11
2.3	Results.....	12
2.4	Discussion	17
2.5	Conclusion remark	21
Chapter 3	A novel blood viscosity estimation method based on pressure-flow characteristics of an oxygenator during cardiopulmonary bypass	22
3.1	Introduction.....	22
3.2	Equation for viscosity estimation.....	23
3.3	Materials and methods	25
3.3.1	Experiments.....	25
3.3.2	Comparison between estimated and measured values of viscosity.....	28
3.3.3	Deemed viscosity using Newtonian fluid parameters	28
3.4	Results.....	29
3.4.1	Accuracy of estimation relative to measurement	29

	3.4.2	Curve-fitting of estimated viscosity and deemed viscosity	33
	3.5	Discussion	36
	3.6	Conclusion remark	40
Chapter 4		A continuous blood viscosity monitoring system for cardiopulmonary bypass applications	41
	4.1	Introduction	41
	4.2	Continuous blood viscosity monitoring system	42
	4.2.1	Signal measurement	44
	4.2.2	Blood viscosity estimation	45
	4.2.3	Display	46
	4.3	Materials and methods	48
	4.3.1	Experimental determination of human blood resistance parameters	48
	4.3.2	Accuracy of estimated viscosity	50
	4.3.3	Robustness improvement following clinical applications	53
	4.4	Results	55
	4.4.1	Resistance parameters of human blood	55
	4.4.2	Correlation between measured and estimated viscosity and Bland-Altman analysis	58
	4.4.3	Optimal window for the algorithm based on clinical applications	62
	4.5	Discussion	67
	4.6	Conclusion remark	71
Chapter 5		Conclusions	73

Bibliography

Acknowledgments

List of figures

- 2.1 Experimental set-up. Input from two transducers, a flowmeter and a thermometer attached to a closed circuit were recorded and displayed on the control panel of a heart lung machine (HLM). VR: venous reservoir; CP: centrifugal pump; FS: flow sensor; TS: thermal sensor; P_{in} : inlet pressure; P_{out} : outlet pressure.
- 2.2 Curve-fitting of pressure-flow characteristics in three different fluids: glycerin solution (a), whole bovine blood (b) and a human RBC suspension (c). fitting of calculated ΔP for the viscosity (η) in three different flows (Q): 2 L/min (a), 4 L/min (b) and 6 L/min (c).
- 2.3 Curve-fitting of calculated ΔP for the viscosity (η) in three different flows (Q): 2 L/min (a), 4 L/min (b) and 6 L/min (c).

- 3.1 Correlation and linear regression analysis of the equation to estimate viscosity (η_e) and viscosity measurement with a VM10-A viscometer (η) with two different flows (Q): 2 L/min (a) and 4 L/min (b).
- 3.2 Bland-Altman plot comparing the two methods for viscosity estimation. The solid line denotes bias (mean of difference), the large dashed line denotes the 95% limits of agreement (two standard deviations of difference), and the small dashed lines denote the 95% confidence interval for the difference between the means.
- 3.3 Correlation and linear regression analysis of the equation to estimate viscosity using Eq. (3.7) (η_{deem}) and viscosity measurement with a VM10-A viscometer (η) with two different flows (Q): 2 L/min (a) and 4 L/min (b).
- 3.4 Curve-fitting of the equation for the estimation of viscosity obtained from estimated viscosity (Eq. (3.6) using bovine blood parameters) and deemed viscosity (Eq. (3.7) using glycerin parameters) for viscosity measurement with a VM10-A viscometer (η) at two different flows (Q): 2 L/min (a) and 4 L/min (b).

- 4.1 Overview of the CPB circuit and system. CP: centrifugal pump; FS: flow sensor; HLM: heart lung machine; P_{in} : inlet pressure; P_{out} : outlet pressure; Q : blood flow; T: Temperature; TS: Thermal sensor; and VR: venous reservoir.

- 4.2 Continuous blood viscosity monitoring system display, with two windows: (a) control panel, in which the upper buttons allow selection of oxygenator and initiation and termination of estimated viscosity monitoring, and (b) monitoring screen, where real-time η_e is displayed at top, trends in η_e , ΔP , and Q over the whole measurement period are displayed in the graphs on the right, and the graphs on the left show the same parameters over the most recent 1200 s.
- 4.3 Pressure gradient ΔP relative to flow Q for a human RBC suspension fitted to two different curves: (a) exponential approximation and (b) linear approximation.
- 4.4 Correlations between and linear regression analysis of the equation used to estimate viscosity η_e and viscosity measured with a VM10-A viscometer η .
- 4.5 Bland-Altman plot comparing estimated and measured viscosity. The solid line denotes bias (mean of difference), the large dashed line denotes the 95% limits of agreement (two standard deviations of difference), and the small dashed lines denote the 95% confidence interval for the difference between the means.
- 4.6 Results of mean value changes in estimated viscosity, hematocrit, and temperature at three points: A, after total CPB has been established; B, after aortic cross-clamp; and C, after declamping.
- 4.7 Relationship between reliability index $\varepsilon_\sigma(\tau)$ averaged over time $\bar{\varepsilon}_\sigma$ and window width N when white Gaussian noise of different standard deviations σ was added to ΔP .
- 4.8 Sample of monitored data during 100 s after initiation of CPB. The graphs show η_e estimated using window width $N = 8$, and ΔP and Q measured from one subject. After initiation of CPB, ΔP increases with increased Q . Although η_e was initially a low value because of dilution with the priming solution, the blood and priming solution mixed 30 s later and were stable. Although estimated η_e showed an almost stable tendency, ΔP and Q were unstable, with amplitudes of approximately ± 5 mmHg and ± 0.5 L/min, respectively.
- 4.9 (a) Correlation between and linear regression analysis of estimated viscosity η_e and measured hematocrit. (b) Correlation between and linear regression analysis of estimated viscosity η_e and measured blood temperature.
- 4.10 Histogram of η_e with bin size of 0.05 mPas; each graph shows a relative frequency for all measurement points, and the percentage value attached on each histogram is

the occurrence ratio of data in the range of 1–3 mPas among all values.

List of table

- 2.1 Coefficients determined for Equation 2.1
- 2.2 Comparison of glycerin solution apparent viscosity with whole bovine blood viscosity
- 2.3 Comparison of glycerin solution apparent viscosity with human RBC suspension viscosity

- 3.1 Measurements for η and ΔP and calculations for η_e

- 4.1 Patient characteristics
- 4.2 Patient characteristics
- 4.3 Coefficients for human RBC suspensions

Chapter 1

Introduction

1.1 Background and purpose

Cardiopulmonary bypass (CPB) was developed in 1953 by Gibbon [1] and is still the only method in cardiac surgery that can be used to obtain a bloodless and motionless operating field. During CPB, the cardiorespiratory function is completely controlled by a heart lung machine (HLM), and blood drained from the right atrium is perfused by a blood pump to the whole body through an oxygenator that enables gas exchange. To substitute for cardiorespiratory function, the maintenance of the oxygen supply-demand balance is critical to the efficacy of the HLM. Therefore, perfusion management focuses on maintaining an appropriate level of hemodilution and temperature based on blood flow [2]–[4], and hemodilution, hemoconcentration, and transfusion are considered acceptable methods for achieving necessary changes to non-physiological hematocrit levels in a short time. Excessive blood temperature decreases, changes in blood pH, and mechanical stress affect the deformability and agglutination of red blood cells (RBCs) [5]. Therefore, it is important to comprehensively measure the influence of non-physiological environmental factors on blood characteristics during the CPB procedure. In this study, we focused on blood viscosity as an index of the blood state variation.

Blood viscosity depends on the deformation and aggregation of RBCs, plasma viscosity, temperature, and hematocrit. Blood is a non-Newtonian fluid with characteristics of pseudoplastic fluids because at a high shear rate, its viscosity

decreases as a result of RBC deformation, and at a low shear rate, its viscosity increases as a result of RBC aggregation [6]. Furthermore, with microcirculation through a diameter of less than 300 μm , the presence of RBCs reduces apparent blood viscosity because of their high deformability, which is termed the Fåhræus-Lindqvist effect [7]. These rheological characteristics of blood are important considerations for maintaining adequate blood flow and oxygen supplies to each organ [7]. The viscoelasticity of blood is also associated with RBC deformability [8]. Ündar *et al.* suggested that in addition to the impacts of hematocrit levels and temperature, other factors involved in CPB also affect blood viscoelasticity, such as the type of membrane in the oxygenator; characteristics of the roller and centrifugal pumps; and mechanical forces of the extracorporeal circuit, cardiomy suction, and pulsatile and nonpulsatile flow [9]. In this regard, influences on blood viscosity during CPB are multifactorial, and information on these factors may be useful for perfusion management.

In cardiac surgery, postoperative cognitive and neurological dysfunction is with an incidence that may exceed 60% and stroke is occurring in 1% to 3% of patients; cerebral embolism and hypoperfusion exacerbated by ischemia/reperfusion injury are believed to be the primary causes of perioperative brain injury [10]. However, because the blood viscosity data during CPB did not intervene in previous clinical outcome studies, it is still unknown how blood viscosity is related to complications that occur during CPB [11]. The diluted blood can increase cerebral blood flow and can change oxygen metabolism [12]. This is a means to offset blood viscosity increase upon a temperature decrease. In contrast, an excessive hematocrit level decreases cerebral blood flow [13]. Hypofunction of red blood cell deformability and red blood cell agglutination due to low shear rate may stop flow because of superabundant viscous

resistance in brain microcirculation [14]. Insufficient heparinization may be accompanied with hyperviscosity and can lead to intravascular thrombosis, procoagulant factor and natural coagulation inhibitor consumption [15]. Despite its potential importance, blood viscosity has not been evaluated because of a lack of technology that can provide simple, continuous, non-contact monitoring. The acquisition of blood viscosity information may also improve perfusion management to minimize neurological complications by monitoring of a viscosity state of the oxygenator flow path, in addition to evaluating the biological effects caused by perfusion during CPB [11]. The objective of this study is to propose the continuous blood viscosity monitoring method for CPB applications.

1.2 Related works

Several studies have proposed methods for monitoring blood viscosity during CPB. Tsuji *et al.* proposed an estimation method for blood viscosity based on Poiseuille's law using the pressure gradient and flow rate of an internal perfusion-type hollow-fiber membrane oxygenator [16]. Because blood is perfused in straight hollow-fiber tubes with a fixed diameter and length through a laminar flow in this oxygenator, the pressure gradient and flow show a linear relationship. The viscosity thus can be calculated by the following Poiseuille's equation (Eq. 1.1):

$$\eta = \frac{\Delta P D^2}{32UL} \tag{1.1}$$

where η [Pas] is the viscosity, ΔP [Pa] is the pressure gradient, L [m] is the fiber

length, U [m/s] is the flow velocity, and D [m] is the hollow-fiber tube diameter.

Present oxygenators, however, are of the external perfusion-type. This type of oxygenator has a low shear stress and pressure gradient for the purpose of suppressing activation of the blood cells, and it is designed to generate a turbulent flow for an effective gas exchange [17], [18]. Therefore, flow paths in external perfusion membrane oxygenators are irregular because the hollow fibers woven into a mat are wound or stacked [19].

Nakamura *et al.* also proposed an estimation method for blood viscosity based on Poiseuille's law using the pressure gradient and flow rate of a hemoconcentrator [20]. However, pressure monitoring is not usually assessed in the blood concentrator at the inlet or outlet. Therefore, a new estimation method is needed for external perfusion oxygenator.

1.3 Outline

The thesis is organized as follows:

In Chapter 2, the author describes the hydrodynamic characteristic of a Newtonian fluid and a non-Newtonian fluid perfusing an external perfusion-type oxygenator. During *in vitro* experiments, one Newtonian fluid (glycerin solution) and two non-Newtonian fluids (whole bovine blood and human red blood cell suspension) are perfused through an oxygenator for three different viscosity levels of each fluid, and their pressure-flow characteristics were examined systematically. The author derives four resistance parameters for the pressure gradient characteristics approximation equation by the least squares method using the relational expression of pressure-flow

characteristics and viscosity.

In Chapter 3, the author proposes a novel equation for estimating viscosity based on the pressure-flow characteristics of the oxygenator. The proposed equation for estimation and monitoring blood viscosity is outlined. Using bovine blood for *in vitro* experiments, the accuracy between the viscosity calculated using the equation and the viscosity measured using a torsional oscillation viscometer are investigated for three hematocrit levels across a given temperature change.

In Chapter 4, the author proposes an algorithm that estimates blood viscosity during CPB and validates its application in a clinical case. First, the author outlines the continuous blood viscosity monitoring system based on the proposed algorithm. Next, the viscosity is estimated using the proposed algorithm and compared with the viscosity measured using a viscometer for 20 patients who underwent mildly hypothermic CPB. The author additionally applies the developed system to 10 patients and reports robustness improvements to the proposed algorithm based on acquired continuously estimated blood viscosity data.

Finally, Chapter 5 concludes the dissertation and outlines related challenges and future work.

Chapter 2

Hydrodynamic characteristics of a membrane oxygenator: modeling of pressure-flow characteristics and their influence on apparent viscosity

2.1 Introduction

Blockage of an oxygenator flow path during CPB results in serious complications. Thus, it is essential to monitor the oxygenator pressure gradient carefully, as it is the only means of detecting a blockage. The pressure gradient largely depends on blood flow and, to a lesser extent, blood viscosity. There are three types of abnormal membrane oxygenator pressure gradients during CPB, two of which are reversible [21]. The reversible abnormal pressure gradient may be caused by a specific increase in viscosity rather than blockage by clots, since blood changes from a liquid into a gel phase during the coagulation process [22] and the deformation and agglomeration of red blood cells (e.g., echinocytes and cold agglutination) cause a severe increase in blood viscosity [23], [24].

In past studies, Tsuji *et al.* proposed an estimate of blood viscosity using Poiseuille's law and the pressure gradient of an internal-perfusion, hollow-fiber oxygenator [16]. Fluids which passed through the straight hollow-fiber tubes influenced the apparent viscosity due to the Fåhræus-Lindqvist effect, related to differences between Newtonian and non-Newtonian fluids. The viscosity obtained from the pressure-flow characteristics

in a membrane oxygenator may help detect factors that change oxygenator resistance, such as the generation of a platelet-fibrin thrombus, erythrocyte deformation, erythrocyte aggregation and plasma viscosity. However, flow paths in external perfusion membrane oxygenators are irregular because the hollow fibers are woven into a mat and are wound or stacked [19]. Moreover, flow paths are further complicated in oxygenators with an integrated arterial filter, making it unclear whether the apparent viscosity changes can be quantified from pressure-flow characteristics in membrane oxygenators. Therefore, the objectives of this study were to model pressure-flow characteristics of a membrane oxygenator with an integrated arterial filter and quantify the influence of non-Newtonian fluids on the apparent blood viscosity.

2.2 Materials and methods

The *in vitro* experiments involved the perfusion of three Newtonian and non-Newtonian fluids through a membrane oxygenator and measuring the pressure gradient and flow to obtain a change in viscosity.

2.2.1 Experiments

- ***Test circuit***

A membrane oxygenator with a 32- μm integrated arterial filter (CAPIOX-FX15; Terumo Cardiovascular Systems Corp., Tokyo, Japan) and an average hollow fiber gap of 100 μm for the passage of blood was used. The oxygenator, venous reservoir (CX-RR40; Terumo Cardiovascular Systems Corp.) and centrifugal pump (MP-23; Senko Medical Instrument Mfg. Co. Ltd., Tokyo, Japan) were connected with 3/8 inch

polyvinyl chloride tubing in order to form a closed circuit; these components comprised the *in vitro* experimental system (Fig. 2.1). A three-way stop-cock was attached to an inlet tube and the oxygenator outlet and pressure was measured through a transducer (DTCL03; Argon Medical Devices Japan, Inc., Tokyo, Japan) from the stop-cock. An ultrasonic blood flowmeter (Transonic H9XL; Transonic Systems Inc., Ithaca, NY, USA) was installed on the exit side tube of the oxygenator. A heat exchanger was connected to the oxygenator and the temperature measured at the oxygenator outlet. The in-out pressures, flow and temperature of the oxygenator were displayed on an artificial heart-lung machine (HAS-2; Senko Medical Instrument Mfg. Co. Ltd.).

- ***Test fluids***

A glycerin solution was used to model a Newtonian fluid while whole bovine blood and a human red blood cell (RBC) suspension (in saline) represented non-Newtonian fluids. If the oxygenator outlet temperature of each fluid perfused through the test circuit was stable at 36 °C, viscosity was adjusted with a torsional oscillation viscometer (VISCOMATE VM-10A; Sekonic Co. Ltd., Tokyo, Japan). Detailed fluid procedures were as follows:

1. Glycerin solution. 97% glycerin was added to water, accumulated in the venous reservoir and then perfused through the circuit. Samples were prepared with 0.89 (0% glycerin), 1.78 (30% glycerin) and 2.96 (40% glycerin) mPas viscosities by dilution with water.
2. Whole bovine blood. Pooled whole bovine blood (DARD Co. Ltd., Tokyo, Japan), including plasma, was maintained by the addition of citric acid (anticoagulant), accumulated in the venous reservoir with 0.9% saline and then perfused through the circuit. Samples with 1.57, 2.69 and 3.52 mPas viscosities were prepared by

hemoconcentration, using a blood concentrator and dilution with 0.9% saline; hematocrits were 19.3%, 31.0% and 39.8%, respectively.

3. Human RBC suspensions. Human RBCs suspended in saline, consisting of expired, irradiated, concentrated, leukocyte-reduced RBCs (without plasma; Japanese Red Cross Society, Tokyo, Japan) were accumulated in the venous reservoir with Albuminar-5 (CSL Behring K.K., Tokyo, Japan) and 0.9% saline and then perfused through the circuit. Samples with 1.88, 2.33 and 2.80 mPas viscosities were prepared by hemoconcentration, using a blood concentrator and dilution with 0.9% saline; hematocrits were 14.1%, 24.5% and 30.7%, respectively.

Each sample of the three test fluids was perfused and circulated through the test circuit at a constant temperature of 36 °C. The rotational speed of the centrifugal pump was increased from 1,000 rpm to 3,500 rpm in 100 rpm intervals approximately every 3 min (after each data recording). The increase of the rotational speed resulted in an increase in the temperature of less than 0.5 °C for all samples. The mean inlet pressure (P_{in}) and outlet pressure (P_{out}) of the oxygenator and flow (Q) of each rotational speed were recorded. The test circuit, including the oxygenator and tubing, was changed for every test fluid.

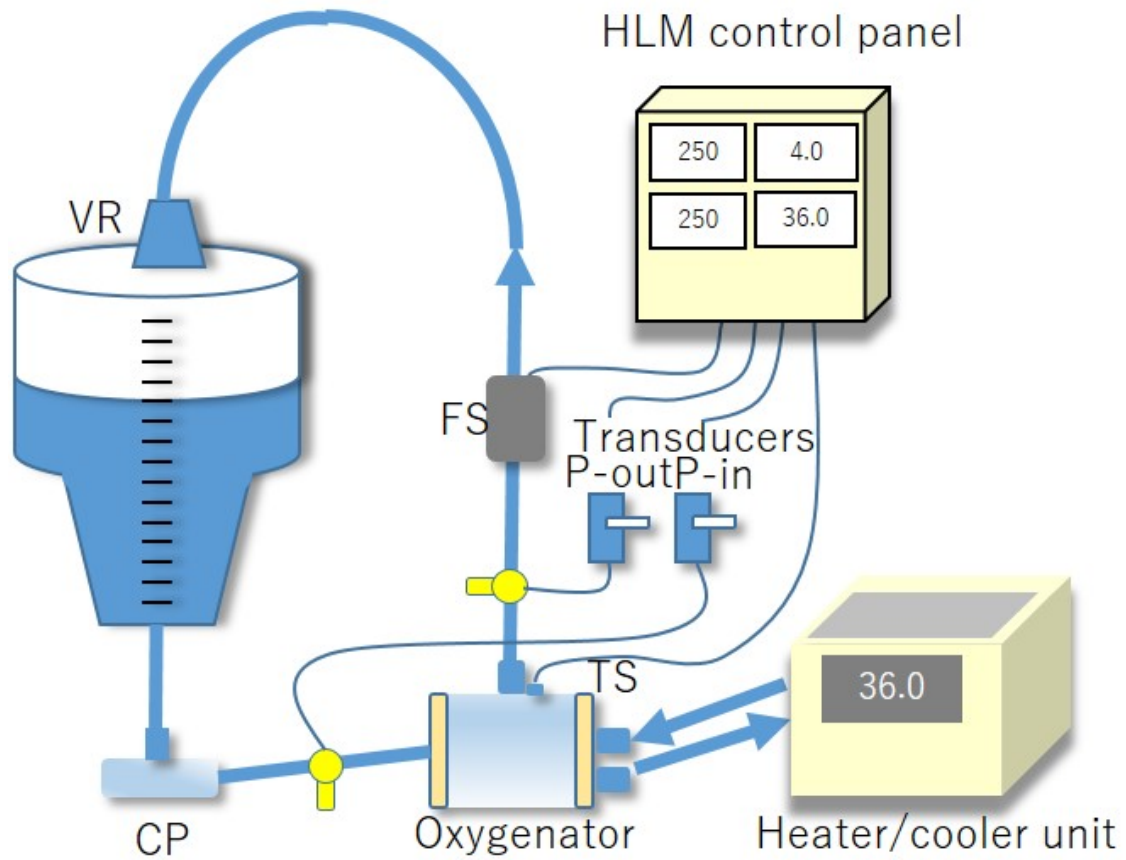


Fig. 2.1 Experimental set-up. Input from two transducers, a flowmeter and a thermometer attached to a closed circuit were recorded and displayed on the control panel of a heart lung machine (HLM). VR: venous reservoir; CP: centrifugal pump; FS: flow sensor; TS: thermal sensor; P_{in} : inlet pressure; P_{out} : outlet pressure.

2.2.2 Pressure gradient characteristics approximation equation

Our proposed pressure gradient characteristics approximation equation (Eq. 2.1) approximates the pressure gradient ($\Delta P = P_{in} - P_{out}$) from Q and the viscosity (η) based on pressure-flow characteristics. The ΔP was calculated from a plot of ΔP versus Q and the relational expressions of Q and ΔP were derived for each sample. Values for the four resistance parameters of Eq. (2.1) were obtained using a non-linear least squares method from the relational expression of pressure-flow characteristics and η . The oxygenator drag coefficients C_r and C_f , decided depending on the characteristics of the fluid, constitute a resistance parameter; other coefficients specific to the oxygenator are the loss coefficient of momentum C_b , which depends on the flow passage shape, and the loss coefficient of momentum C_a , which is decided depending on the characteristics of the fluid.

$$\Delta P = (C_r\eta + C_f)Q^{C_b \exp(C_a\eta)}. \quad (2.1)$$

2.2.3 Simulations with approximation equation

The ΔP calculated from Eq. (2.1) was simulated using the same Q and η for the three test fluids. The ΔP of each fluid was calculated at each Q (2, 4 and 6 L/min) and the η for each fluid was plotted versus ΔP . ΔP was assessed as a change occurring only under the influence of the apparent viscosity (η_{app}) of each fluid. The η_{app} was obtained when characteristics of the glycerin solution were assumed for bovine blood and the RBC suspension in Eq. (2.1). The ΔP for each Q (2, 4 and 6 L/min) and each η (2, 3 and 4 mPas) in bovine blood and the RBC suspension were calculated. The η_{app} was determined as the point where a vertical line drawn from the calculated ΔP intersected

with the glycerin solution curve (Fig. 2.2).

2.3 Results

Fig. 2.2 shows pressure-flow characteristics of the glycerin solution, bovine blood and human RBC suspension. A non-linear Q to ΔP was observed with a coefficient of determination of almost 1 by exponential approximation. The resistance parameters of Eq. (2.1), indicating the relationship between Q and ΔP for each fluid, were derived by the non-linear least squares method (Table 2.1); bovine blood has the highest C_r of the three fluid types tested; C_f was close to 0 for the glycerin solution, C_b was similar for all fluids and C_a was almost the same for bovine blood and the RBC suspension.

Results of the simulation of ΔP calculated from Eq. (2.1) for the three test fluids are shown in Fig. 2.3. At $Q = 2$ L/ min, the ΔP in the η range of 1-4 mPas was 7-60 mmHg for bovine blood and the RBC suspension, while the ΔP of the glycerin solution was approximately 20-70 mmHg (Fig. 2.2a). At $Q = 4$ L/min, the bovine blood and RBC suspension ΔP were approximately 20-120 mmHg and the glycerin solution ΔP was 60-160 mmHg (Fig. 2.2b). At $Q = 6$ L/min, the ΔP of bovine blood and the RBC suspension were approximately 30-200 mmHg, while the glycerin solution ΔP was approximately 100-250 mmHg (Fig. 2.2c). At all Q , the glycerin solution had a ΔP around 10-70% compared with bovine blood and the RBC suspension. Though the bovine blood and RBC suspension showed a similar trend when $Q = 2$ L/min, bovine blood tended to have a higher ΔP when η was high. Tables 2.2 and 2.3 show the η_{app} when the ΔP of bovine blood and the RBC suspension were applied to the glycerin solution. Compared to the glycerin solution, the η_{app} was low in bovine blood

(10%-44%) and the RBC suspension (35%).

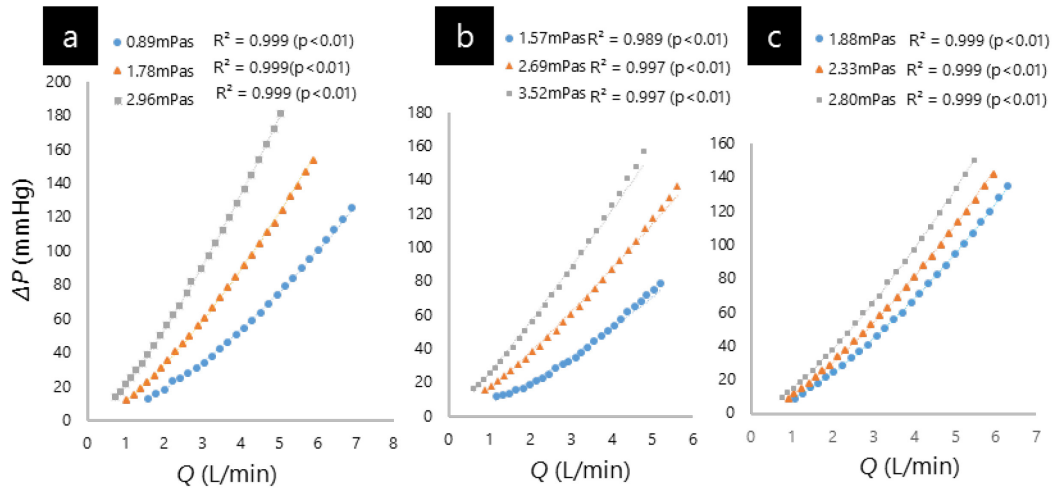


Fig. 2.2 Curve-fitting of pressure-flow characteristics in three different fluids: glycerin solution (a), whole bovine blood (b) and a human RBC suspension (c).

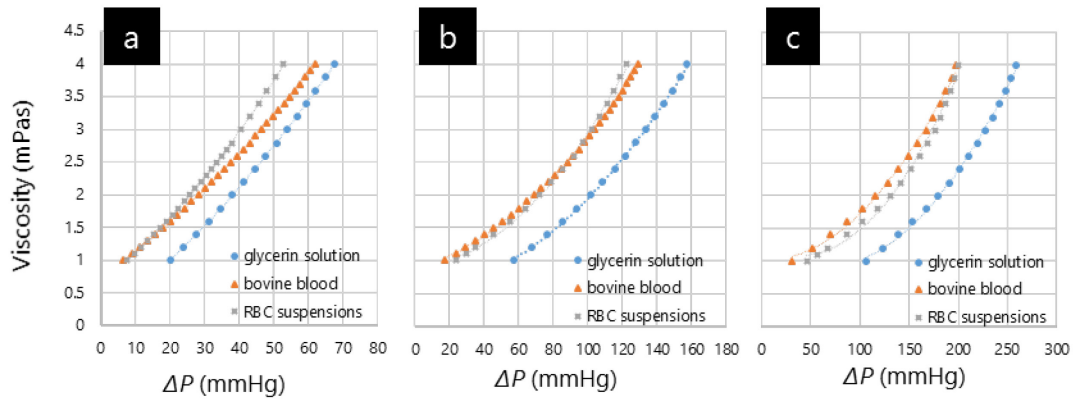


Fig. 2.3 Curve-fitting of calculated ΔP for the viscosity (η) in three different flows (Q): 2 L/min (a), 4 L/min (b) and 6 L/min (c).

Table 2.1 Coefficients determined for Equation 2.1

Resistance parameters	C_r	C_f	C_b	C_a
Glycerin solution	7.2978	-0.3285	1.6317	-0.072
Bovine Blood	9.7638	-6.6795	1.5643	-0.105
RBC suspensions	6.7443	-4.2659	1.8024	-0.099

Table 2.2 Comparison of glycerin solution apparent viscosity with whole bovine blood viscosity

Q	ΔP (mmHg)	η (mPas)	η_{app} (mPas)	η/η_{app}
2 L/min	28.2	2.00	1.43	0.72
	46.4	3.00	2.52	0.84
	62.0	4.00	3.59	0.90
4 L/min	68.7	2.00	1.23	0.61
	104.0	3.00	2.08	0.69
	128.9	4.00	2.84	0.71
6 L/min	115.7	2.00	1.11	0.56
	166.9	3.00	1.80	0.60
	197.9	4.00	2.24	0.56

Q : flow; ΔP : pressure gradient (i.e., pressure change); η : viscosity; η_{app} : apparent viscosity.

Table 2.3 Comparison of glycerin solution apparent viscosity with human RBC suspension viscosity

Q	ΔP (mmHg)	η (mPas)	η_{app} (mPas)	η/η_{app}
2 L/min	25.7	2.00	1.30	0.65
	40.4	3.00	2.15	0.72
	52.7	4.00	2.94	0.74
4 L/min	71.7	2.00	1.29	0.65
	102.2	3.00	2.03	0.68
	122.1	4.00	2.61	0.65
6 L/min	130.5	2.00	1.29	0.65
	176	3.00	1.94	0.65
	199.6	4.00	2.37	0.60

Q : flow; ΔP : pressure gradient (i.e., pressure change); η : viscosity; η_{app} : apparent viscosity.

2.4 Discussion

In this study, the pressure-flow characteristics of three fluids flowing through an oxygenator with an integrated arterial filter were examined systematically, relative to various η . Due to the non-linear relationship of the oxygenator flow path in this study, fitting Q to Poiseuille's law was difficult. The external perfusion membrane oxygenator was designed with a complicated flow path to reduce the ΔP and improve gas exchange by fitting it to an exponential relation. Thus, the non-linear pressure-flow characteristics observed in this oxygenator were modelled as a pressure gradient approximation equation (Eq. 2.1). Four resistance parameters, each specific to the oxygenator, were derived for use with Eq. (2.1), but their derivation is possible and similar regardless of manufacturer. In particular, we previously fitted pressure-flow characteristics of three types of membrane oxygenators to exponential relations [25]. If resistance parameters were $C_f = 0$, $C_b = 1$, and $C_a = 0$, the pressure-flow relations approached Poiseuille's flow; if $C_b = 2$, the momentum loss due to the whirlpool became the major Q effect. In this study, pressure-flow characteristic results obtained for the glycerin solution were closest to a Poiseuille flow, while the RBC suspension had the most momentum loss.

The simulation with Eq. (2.1) was used to confirm the influence of each fluid on η . Although η and Q were the same for each test fluid, it is thought that the decreasing ΔP of the non-Newtonian fluids (whole bovine blood and human RBC suspension) was due to a decrease in η_{app} . Moreover, the Newtonian fluid (glycerin solution) was not influenced by η_{app} under any of the flow situations. Therefore, a change in η_{app} pressure-flow characteristics of the glycerin solution was observed when the Q and ΔP of the other fluids were the same.

The decrease in η_{app} may be possible for two reasons. In microcirculation through a

diameter of 300 μm or less, the presence of RBCs reduces the η , termed the Fåhræus-Lindqvist effect [7]. Until now, the assessment of the fluid properties of blood during microcirculation and the Fåhræus-Lindqvist effect has only been investigated using straight tube models [26]. Cell migration forms a layer of plasma absent of RBCs and is related to a reduction of blood η_{app} [27]. We assumed a similar effect in our human RBC suspension because a cell-free layer formed with our external perfusion membrane oxygenator when samples were perfused through the hollow fibers. According to Pries *et al.* [28], an approximate 15% decrease in η_{app} occurs when the oxygenator flow tract tube gap is, on average, 100 μm in diameter.

Second, fluidity increases when shear is added to a fluid. In blood, the η_{app} decreases conspicuously until shear rates exceed 50 s^{-1} and further increases in shear rate have little effect [29]. Because the shear rate of the oxygenator was approximately 30 s^{-1} at $Q = 5$ L/min, only a slight influence on η_{app} was observed. Moreover, the different Q had almost no influence on the rate of η_{app} change. Therefore, the non-Newtonian fluid flowing in the oxygenator did not seem to influence the changes in Q .

Additionally, a torsional oscillation viscometer was used for actual measurement of η in this study. This viscometer, based on piezoelectric torsional oscillation technology, can measure the η dynamically under static conditions. When the yield stress is exceeded, static blood has a stress-shear rate function under creeping flow conditions closely following Casson's model [30]. Our results suggest bovine blood and the RBC suspension possess yield stress. However, Travagli *et al.* reported that the torsional oscillation viscometer gave approximately 20% higher η than the cone-plate viscometer with low shear rates (25 s^{-1}) in human blood η [31]. It is possible that static blood η measured by a torsional oscillation viscometer may decrease the η_{app} by approximately

20% at low shear rates due to the flow. Thus, we posited that an η_{app} difference of around 35% was observed in both Newtonian and non-Newtonian fluids perfused through our oxygenator.

Furthermore, the influence of η_{app} on Newtonian and non-Newtonian fluids was quantified in our study by differences in ΔP . The potential for the derivation of new technology by elucidating hydrodynamic characteristics of membrane oxygenators relies on estimates of η . This technology has clinical importance as a method for condition monitoring of the oxygenator. During CPB, blood flow and the blood viscosity change pressure gradients under various situations and, therefore, the pressure gradient cannot be used alone for direct condition monitoring of the oxygenator. In addition, the influence of blood viscosity varies, depending on the type of blood pump used. For example, when blood viscosity increases, the pressure gradient rises with the roller pump and blood flow decreases with the centrifugal pump. Because blood viscosity in the oxygenator is a physical quantity derived by blood flow and pressure gradient, we can continuously monitor viscosity changes in the oxygenator regardless of the type of pump used. Therefore, it provides sensitive monitoring of reversible erythrocyte agglutination and may detect the irreversible abnormal value as blockage of the oxygenator flow path.

Finally, the model proposed in this chapter may be applied to translational research of the CPB components, including other types of oxygenators as well as pediatric ones. Since pressure-flow characteristics depended on the kind of the fluid, tests using Newtonian fluid as a priming solution may cause an incorrect evaluation on the influence of viscosity.

This study has limitations. Since the viscometer used for the experiments did not

have a temperature control function, the sample temperature was not maintained at the oxygenator. Therefore, the viscosity of the water at 36 °C in the oxygenator outlet was different from the theoretical value. However, for relative comparisons of each fluid, all the samples were measured at room temperature, using the same method and measurement time. It is also known that a centrifugal pump becomes a source of heat in a circuit [32]. In this study, the increase in the number of rotations of the centrifugal pump resulted in temperature changes less than 0.5 °C for all samples. It must be investigated how the change of temperature that a difference of size and structure of centrifugal pump causes influences viscosity.

Since the required volume (approximately 1000 mL) of whole human blood, including plasma, was hard to obtain, it was not used in this study. Therefore, the influence of plasma η on RBC suspensions was not evaluated. Human plasma η is usually considered a Newtonian fluid [33]. However, it has been suggested that it may behave as a non-Newtonian fluid in patients with abnormally elevated plasma protein levels [34]. In fact, differences in resistance characteristics were found between the whole bovine blood (with plasma) and the human RBC suspension (without plasma) in this study, warranting further investigation. Therefore, future studies should examine, in greater detail, the effect of bovine versus human RBCs with and without plasma, as well as where/when the presumed Fåhræus-Lindqvist effect occurs along the oxygenator flow path. Nevertheless, results obtained from this analysis of membrane oxygenator pressure-flow characteristics support the need for continuous η monitoring during CPB.

2.5 Conclusion remark

This study demonstrated that the pressure-flow characteristics of both Newtonian and non-Newtonian fluids fitted exponential relations in a membrane oxygenator with an integrated arterial filter. Hydrodynamic characteristics were modelled, quantified and shown to influence the η_{app} of the tested non-Newtonian fluids. Therefore, this study shows the potential of estimating η from mathematical relations of ΔP and Q . By continuously monitoring the estimated η via measured oxygenator pressure-flow characteristics, early detection of oxygenator blockages and/or failure may be possible.

Chapter 3

A novel blood viscosity estimation method based on pressure-flow characteristics of an oxygenator during cardiopulmonary bypass

3.1 Introduction

In Chapter 2, we modeled pressure-flow characteristics using an oxygenator of the external perfusion type for three fluids (glycerin solution, whole bovine blood, and human RBC suspensions) and quantified how viscosity of the fluids were affected by this device. However, the viscosity of fluid was measured by a viscometer and could not be estimated from measurements of pressure and flow. In this chapter, a novel technique is proposed in order to estimate blood viscosity in the oxygenator based on its pressure-flow characteristics. This method estimates viscosity based on pressure and flow information without the need for any additional sensors and provides a method for monitoring blood viscosity continuously.

On the other hand, determination of the four parameters included in the model required the use of blood of over 1000 ml by experiments for each oxygenator type and their experimental circuits, thereby creating high costs of calibration. Above all, use of human blood for the experiment is difficult ethically. Therefore, we also propose a new method for blood viscosity monitoring that approximates the pressure-flow characteristics of blood considered as a non-Newtonian fluid with characteristics of a Newtonian fluid by using parameters derived from glycerin solution to enable ease of

acquisition. Although this method cannot estimate the absolute viscosity of blood, it may prove useful in the detection of blockage in an oxygenator flow path, as a relative means of monitoring of the blood viscosity variation of the perfusing oxygenator. The objective of this chapter is to demonstrate the methods proposed here, in which hematocrit levels and temperature were systematically adjusted via *in vitro* experiments and used to evaluate our proposed viscosity estimation method.

3.2 Equation for viscosity estimation

In Chapter 2, the oxygenator pressure gradient ($\Delta P = P_{in} - P_{out}$) was modeled on a pressure gradient characteristic approximation equation (Eq. 3.1) that is based on η and Q . Eq. (3.1) approximates ΔP from Q and η based on pressure-flow characteristics, and values for the four resistance parameters of Eq. (3.1) were obtained using a non-linear least squares method from the relational expression of pressure-flow characteristics of a certain fluid including whole bovine blood that perfused the oxygenator and η . The four resistance parameters are coefficients specific to the FX15 oxygenator and are not dependent on temperature or hematocrit levels. The oxygenator drag coefficients C_r and C_f are dependent on the characteristics of the fluid that constitute a resistance parameter, while other coefficients specific to the oxygenator include the loss coefficient of momentum C_b , which depends on the shape of the passage, and the loss coefficient of momentum C_a , which depends on fluid characteristics.

$$\Delta P = (C_r \eta + C_f) Q^{C_b \exp(C_a \eta)}. \quad (3.1)$$

Eq. (3.1) is derived as follows. Because the pressure-flow characteristics in the

oxygenator perfused with three fluid samples (viscosities of 1, 2, and 3 mPas, respectively) fitted well with the power approximation curve, each sample η can be expressed using in the form of Eq. (3.2).

$$\Delta P = RQ^A. \quad (3.2)$$

R is determined using Eq. (3.3):

$$R = C_r\eta + C_f \quad (3.3)$$

where the parameters C_r and C_f are determined by a linear regression using the least-squares method. In addition, an exponential relationship between A and η is also determined using the least-squares method, yielding Eq. (3.4) as a general expression.

$$A = C_b \exp C_a \eta. \quad (3.4)$$

Finally, substituting Eqs. (3.3) and (3.4) into Eq. (3.2) yields Eq. (3.1). With each resistance parameter derived beforehand, the only unknown quantity after measurement of P_{in} , P_{out} , and Q is η . Therefore, we derived the solution in which $f(\eta_e)$, where η_e represents estimated viscosity, is assumed to be 0 using the Newton-Raphson method to calculate the estimated viscosity, η_e [35].

$$f(\eta_e) = \Delta P - (C_r\eta_e + C_f)Q^{C_b \exp(C_a \eta_e)}. \quad (3.5)$$

It should be noted that a set of parameters, C_a , C_b , C_f , and C_r , specified for the given oxygenator and fluid can estimate η_e from the measured P_{in} , P_{out} , and Q without using temperature and hematocrit levels. The parameters set for the three fluids corresponding to the FX15 oxygenator derived in Chapter 2 are given in Table 2.1. According to values listed in Table 2.1, the equation for the estimation of viscosity using the resistance parameter of bovine blood is Eq. (3.6):

$$f(\eta_e) = \Delta P - (9.7638\eta_e - 6.6795)Q^{1.5643\exp(-0.105\eta_e)}. \quad (3.6)$$

Let us consider a viscosity estimation for bovine blood using the resistance parameters of the glycerin solution. In other words, the pressure-flow characteristics of bovine blood considered as a Newtonian fluid is approximated with the characteristics of the glycerin solution. The equation for estimating approximated viscosity using the resistance parameters of the glycerin solution is expressed as (3.7):

$$f(\eta_{deem}) = \Delta P - (7.2978\eta_{deem} - 0.3285)Q^{1.6317\exp(-0.072\eta_{deem})}. \quad (3.7)$$

In this paper, the approximated viscosity is expressed as deemed viscosity (η_{deem}).

3.3 Materials and methods

3.3.1 Experiments

For the *in vitro* experiments, three samples of whole bovine blood with different

hematocrit levels (21.8%, 31.0%, and 39.8%) were prepared to represent most common hematocrit levels encountered during CPB. The samples were perfused into a membrane oxygenator that had a 32 μm integrated artery filter (CAPIOX-FX15; Terumo Cardiovascular Systems Corp., Tokyo, Japan) and an average hollow fiber gap of 100 μm for blood passage. The oxygenator, venous reservoir (CX-RR40; Terumo Cardiovascular Systems Corp.), and centrifugal pump (MP-23; Senko Medical Instrument Mfg. Co., Ltd., Tokyo, Japan) were connected with a 3/8 inch polyvinyl chloride tubing to form a closed circuit. A three-way stopcock was attached to an inlet tube and the oxygenator outlet and pressure was measured through a transducer (DTCL03; Argon Medical Devices Japan, Inc., Tokyo, Japan) at the stopcock. An ultrasonic blood flowmeter (Transonic H9XL; Transonic Systems Inc., Ithaca, NY, USA) was installed on the oxygenator exit side tube. A heat exchanger was connected to the oxygenator, and the temperature was measured at the oxygenator outlet. The in-out pressures, flow, and temperature of the oxygenator were displayed on an HLM (HAS-2; Senko Medical Instrument Mfg. Co., Ltd.) (Fig. 2.1).

Fresh whole bovine blood (~1000 mL, DARD. Co., Ltd., Tokyo, Japan) at a final concentration of 0.45 w/v% containing sodium citrate in 10% of all volume for anticoagulation was used. The samples maintained more than 1,000 s of the activated clotting time and continued achieving anticoagulation during the experiment. It should be noted that although blood viscosity changes slightly due to the addition of anticoagulant to blood, changed viscosity must be estimated because blood of patients will be fully anticoagulated during a clinical CPB. Pooled bovine blood, including plasma, was accumulated in the venous reservoir with 0.9% saline and then perfused through the circuit. Samples with hematocrit levels of 21.8%, 31.0%, and 39.8% were

prepared by hemoconcentration using a blood concentrator and dilution with 0.9% saline. Each sample was used to perfuse the test circuit while maintaining an initial temperature of 37 °C.

The oxygenator mean inlet pressure (P_{in}) and outlet pressure (P_{out}) were recorded for a flow (Q) of 2 L/min. When the rotational speed of the centrifugal pump was increased and the flow reached 4 L/min, P_{in} and P_{out} were again recorded. After these measurements were completed, the blood temperature was lowered by increments of 2 °C from 37 °C and viscosity (η), P_{in} and P_{out} , at 2 L/min and 4 L/min were measured, with similar results obtained until 27 °C.

When P_{in} and P_{out} at 2 L/min were recorded at each temperature, 3 mL of bovine blood were obtained from the circuit and the η was measured with a torsional oscillation viscometer (VISCOMATE VM-10A; Sekonic Co., Ltd., Tokyo, Japan). This viscometer is a torsional oscillation viscometer characterized by constant shear stress systems driven by a piezoelectric ceramic source. The viscometer can measure viscosity by sensing a change in oscillation amplitude of a liquid-immersed detector, based on constant input voltage [31]. The frequency of applied oscillation was 500 Hz. The angular acceleration of the detector was measured and reported as a dynamic viscosity with a declared range of 0.400 mPas–1000 mPas and a precision equal to $\pm 5\%$. The cylindrical probe diametrical dimension was 9 mm. The blood was immediately placed into a sample cup and measured under static conditions. For η measurements, temperature was monitored during each measurement by means of sample cups placed in a water bath equilibrated to the temperature corresponding to the sample at room temperature (28 °C). The η was recorded 10 seconds from the start of the measurement. In these measurements, the difference in temperature between that displayed by the

HLM and the sample cup ranged from 0.3 °C to 1.3 °C.

The measurement was comprised of 36 points with measurements for each time point at each of three hematocrit levels, six temperature levels, and two flow levels. As for all data, Q , P_{in} and P_{out} were measured under stable conditions. It should be noted that the estimated viscosity did not vary under stable conditions, i.e. its standard deviation was zero, and only one sample for each measurement was used in this paper.

3.3.2 Comparison between estimated and measured values of viscosity

The η_e of bovine blood was calculated using Eq. (3.6) with ΔP obtained at each temperature of each sample for both Q values (2 L/min, 4 L/min) and this value was plotted as a function of η . The systematic errors and compatibility between methods were assessed using Bland-Altman analysis. Statistical analysis was performed using XLSTAT software and JMP 11.0 (SAS Institute Japan Ltd., Tokyo, Japan) was used for regression analysis and Bland-Altman plotting.

3.3.3 Deemed viscosity using Newtonian fluid parameters

Independently of its estimated viscosity η_e , the deemed viscosity was similarly calculated from Eq. (3.7), incorporating the parameters of the glycerin solution. The resulting deemed viscosity was plotted as a function of measured viscosity. These results and those calculated from Eq. (3.6) were plotted together to determine the influence of the deemed viscosity. The correlations between estimated and deemed viscosities were investigated. Statistical analysis was performed using XLSTAT software for regression analysis.

3.4 Results

3.4.1 Accuracy of estimation relative to measurement

Table 3.1 show η and ΔP obtained from the experiments and η_e calculated from Eq. (3.6). The graph of η derived from the relationship between results obtained from the VM-10A viscometer and η_e as described by Eq. (3.6) is shown in Fig. 3.1a and 3.1b for two different Q values. The parameters η_e and η were strongly correlated in all samples ($R^2 = 0.992$, $p < 0.001$). Fig. 3.2 shows a plot of the Bland-Altman analysis, which revealed a mean bias of -0.026 mPas, a standard deviation of 0.071 mPas, limits of agreement of -0.114 mPas to 0.166 mPas, and a percent error of 5.2%. There was no fixed bias or proportion bias for the viscosity.

Table 3.1 Measurements for η and ΔP and calculations for η_e

	Q	Hematocrit	37 °C	35 °C	33 °C	31 °C	29 °C	27 °C
η (mPas)	—*	21.8%	1.80	1.86	1.87	1.92	1.96	1.98
		31.0%	2.36	2.41	2.47	2.54	2.57	2.68
		39.8%	3.46	3.59	3.71	3.83	3.93	4.03
ΔP (mmHg)	at 2L/min	21.8%	26	28	29	30	31	32
		31.0%	36	37	38	40	41	43
		39.8%	56	59	61	63	64	65
	at 4L/min	21.8%	63	66	68	71	74	76
		31.0%	84	87	90	93	95	98
		39.8%	119	124	128	132	135	139
η_e (mPas)	at 2L/min	21.8%	1.77	1.86	1.91	1.95	2	2.05
		31.0%	2.25	2.3	2.35	2.46	2.51	2.62
		39.8%	3.36	3.55	3.67	3.87	3.93	4
	at 4L/min	21.8%	1.74	1.81	1.85	1.92	1.99	2.03
		31.0%	2.23	2.31	2.39	2.47	2.53	2.62
		39.8%	3.32	3.52	3.69	3.88	4.02	4.22

η : Viscosity measured by VM10-A viscometer; ΔP : oxygenator pressure gradient; Q : blood flow; η_e : Estimated viscosity from Eq. (3.6). * η does not depend on Q .

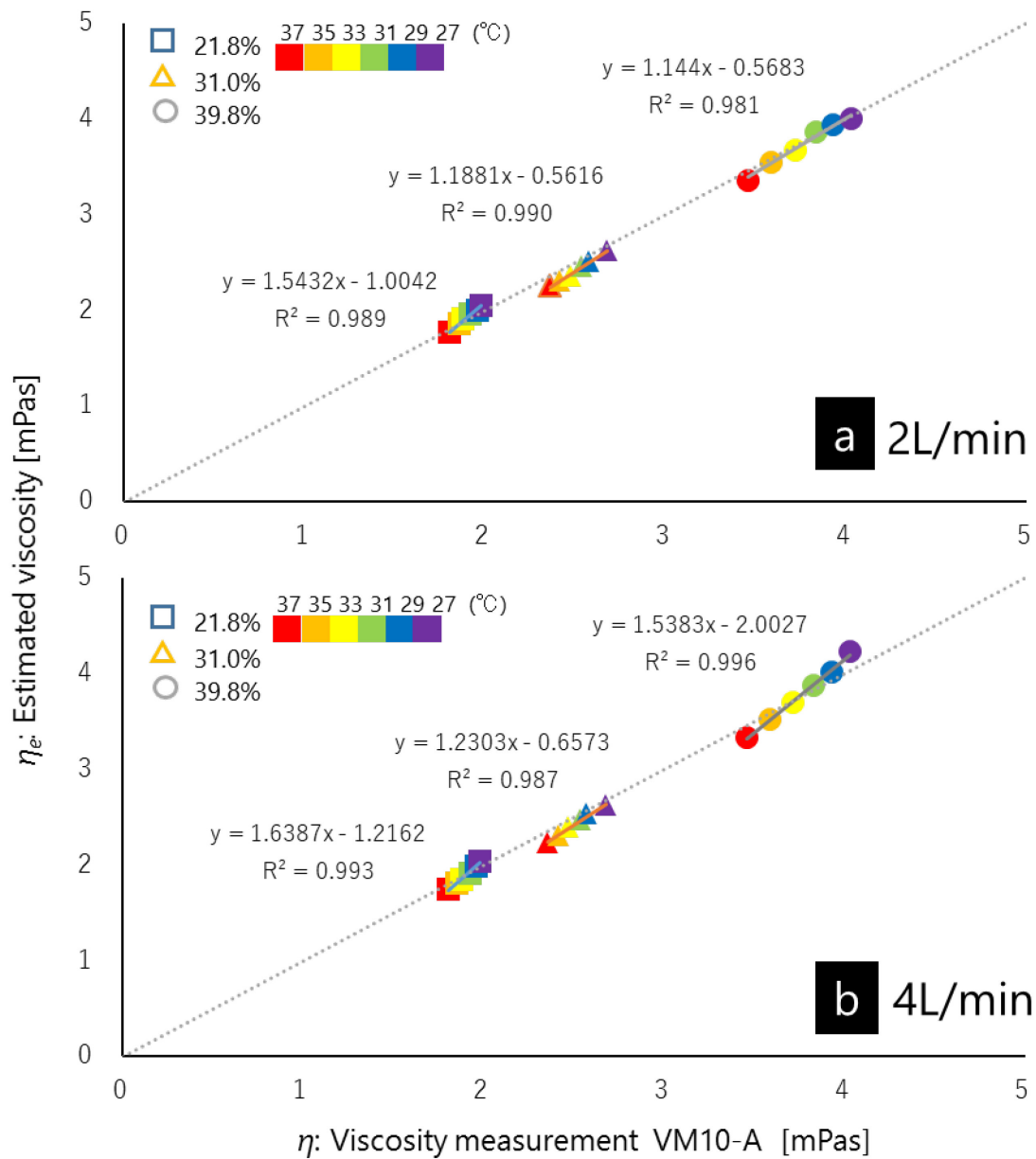


Fig. 3.1 Correlation and linear regression analysis of the equation to estimate viscosity (η_e) and viscosity measurement with a VM10-A viscometer (η) with two different flows (Q): 2 L/min (a) and 4 L/min (b).

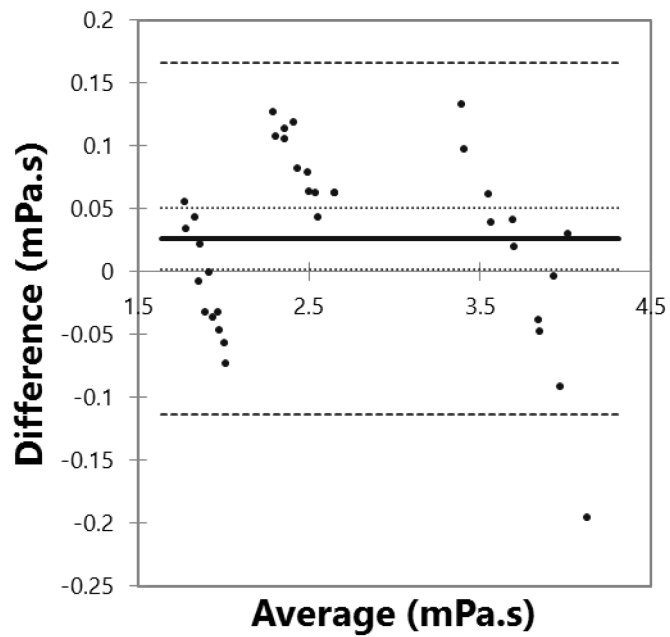


Fig. 3.2 Bland-Altman plot comparing the two methods for viscosity estimation. The solid line denotes bias (mean of difference), the large dashed line denotes the 95% limits of agreement (two standard deviations of difference), and the small dashed lines denote the 95% confidence interval for the difference between the means.

3.4.2 Curve-fitting of estimated viscosity and deemed viscosity

The viscosity graphs derived from the relationship between results obtained using the VM-10A viscometer and deemed viscosity as described by Eq. (3.7) are shown in Fig. 3.3a and 3.3b for the two different Q values. The deemed viscosity and measured viscosity demonstrated a very strong correlation in all samples ($R^2 = 0.918$, $p < 0.001$).

The graphs of measured viscosity vs. estimated viscosity, and measured viscosity vs. deemed viscosity obtained from Eq. (3.6) and (3.7), respectively, are shown in Fig. 3.4. The value of deemed viscosity calculated with Eq. (3.7) was lower than estimated viscosity calculated with Eq. (3.6) by 20–33% at 21.8% hematocrit, 12–27% at 31.0% hematocrit, and 10–15% at 39.8% hematocrit. Furthermore, deemed viscosity was lower than estimated viscosity by 10–30% at 2 L/min and 30–40% at 4 L/min. Estimated viscosity and deemed viscosity had a strong correlation in all samples ($R^2 = 0.913$, $p < 0.001$).

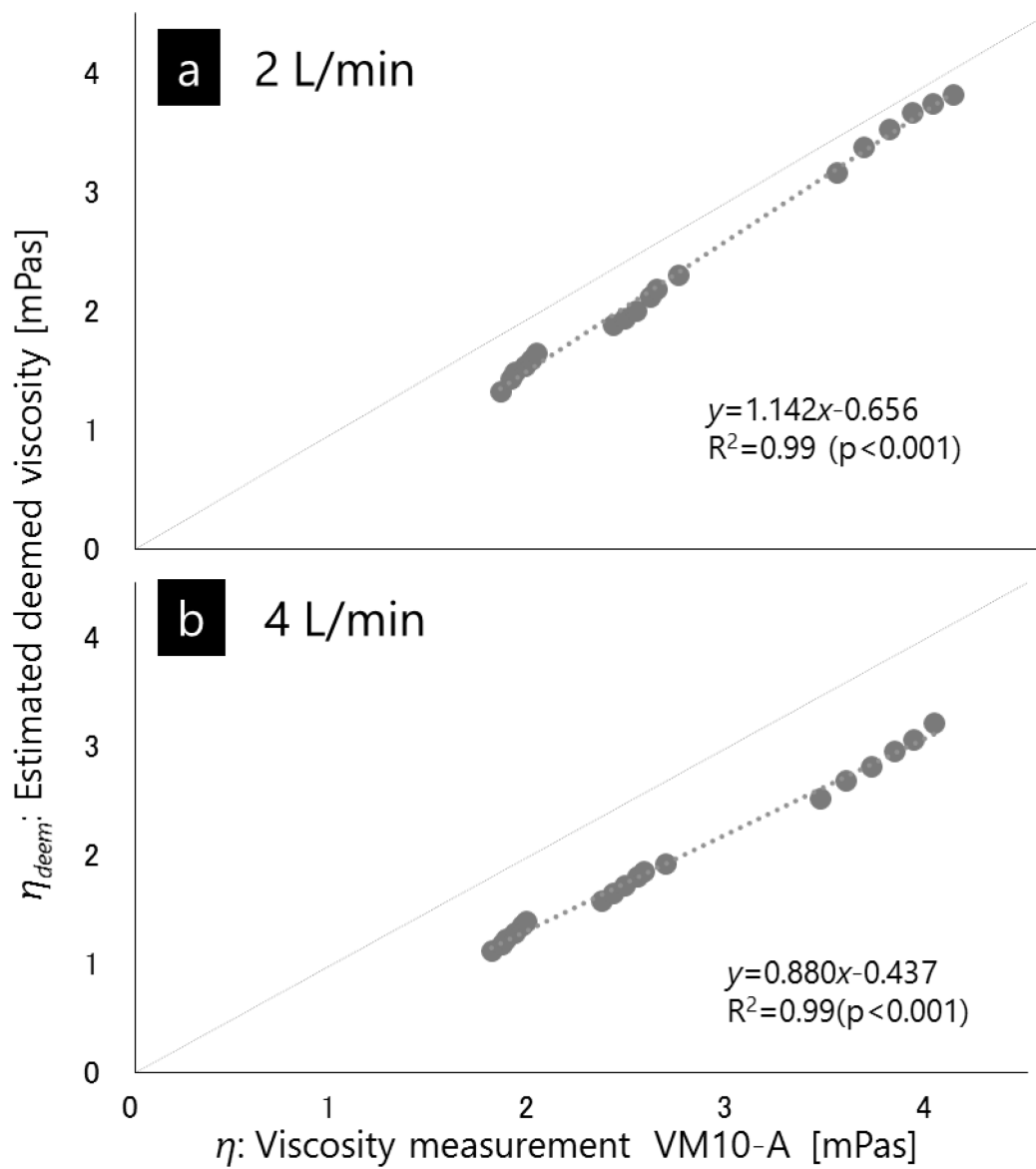


Fig. 3.3 Correlation and linear regression analysis of the equation to estimate viscosity using (3) (η_{deem}) and viscosity measurement with a VM10-A viscometer (η) with two different flows (Q): 2 L/min (a) and 4 L/min (b).

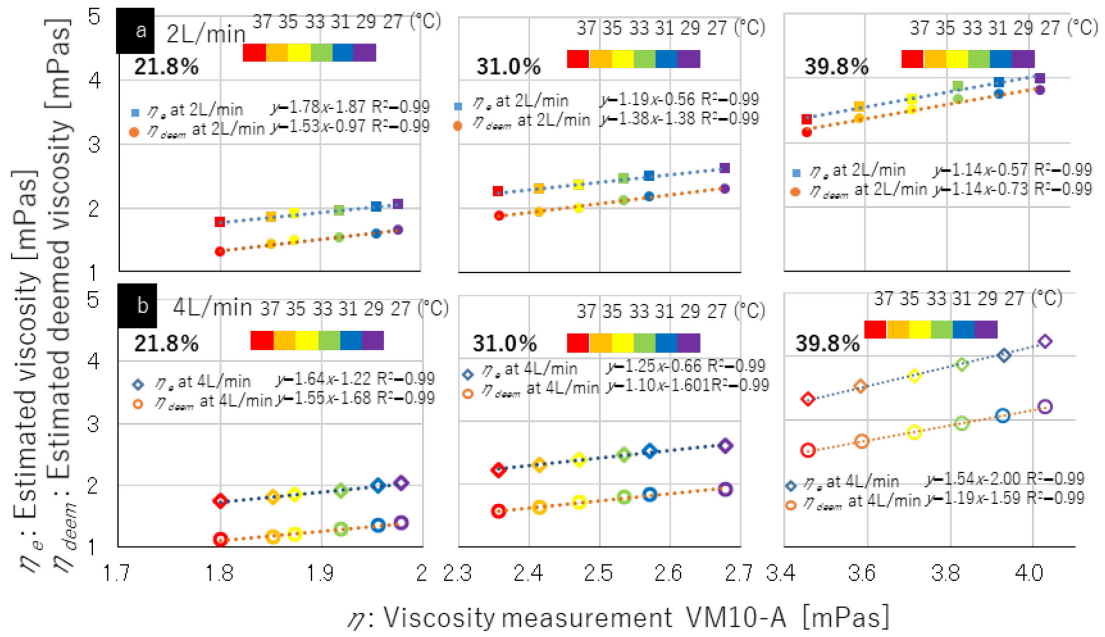


Fig.3.4 Curve-fitting of the equation for the estimation of viscosity obtained from estimated viscosity (Eq. (3.6) using bovine blood parameters) and deemed viscosity (Eq. (3.7) using glycerin parameters) for viscosity measurement with a VM10-A viscometer (η) at two different flows (Q): 2 L/min (a) and 4 L/min (b).

3.5 Discussion

In this study, we proposed an equation to estimate blood viscosity based on pressure and flow information from an oxygenator. The equation and the parameters used for viscosity estimation were modeled based on the differences in viscosity due to hematocrit levels, and four resistance parameters that depend on the oxygenator and fluid were derived for this experiment using the FX15 oxygenator and bovine blood. During CPB, changes in viscosity are primarily due to changes in hematocrit levels and blood temperature [21]. Therefore, the effectiveness of the proposed method was evaluated regarding changes in a clinical range of hematocrit levels during moderate hypothermia. For each sample, estimated viscosity (η_e) was compared to measured viscosity (η) at every temperature change. All samples had a decision coefficient of just less than 1. Results from this method and those from a torsional oscillation viscometer, which has a measurement accuracy of approximately $\pm 5\%$, were then compared. Given that the ratio of the limits of agreement for the average η was 5%, the two methods appear to be comparable.

The selection of the viscometer is important because blood viscosity depends not only on blood sample characteristics but also on the measurement method. Since the torsional oscillation viscometer measures viscosity dynamically, η_e is estimated as a viscosity value depending on this method in this study. In previous clinical studies [36], a rotational viscometer was used to measure blood viscosity to determine rheological characteristics of blood. However, it was unsuitable for determining constant viscosity because the measurement results of the blood viscosity depended on shear rate in this type of viscometer. In contrast, a torsional oscillation viscometer was available for constant viscosity measurements independent of shear rate [37]; it has similar results to

the rotational viscometer at shear rate of 10 s^{-1} [31]. For this reason, the resistance parameters to be used in the equation to estimate viscosity were derived from viscosity values obtained with a torsional oscillation viscometer.

We also proposed deemed viscosity for blood viscosity monitoring that approximates the pressure-flow characteristics of blood considered as a non-Newtonian fluid with characteristics of a Newtonian fluid by using parameters derived from glycerin solution to enable ease of acquisition. Deemed viscosity was compared with estimated viscosity for different hematocrit and flow levels during temperature variation. As the temperature of each sample decreased, the estimated and deemed viscosities increased at a similar rate. Therefore, deemed viscosity values acquired using glycerin parameters may be capable of effectively monitoring relative viscosity changes of blood in a perfusing oxygenator.

Apparent viscosity, which is defined as the ratio of shear stress applied to a fluid to the shear rate, is important for non-Newtonian fluids, including the RBCs [7] that flow through the membrane oxygenator. They are influenced by the Fåhræus-Lindqvist effect, and shear thinning is possible. In chapter 2, we observed the effect of apparent viscosity during flow through the oxygenator in terms of differences of pressure between a Newtonian fluid (glycerin solution) and a non-Newtonian fluid (whole bovine blood) that were expressed as ΔP . Although η and Q were the same for each test fluid, decreases in ΔP of non-Newtonian fluids may result from a decrease in the apparent viscosity. Moreover, Newtonian fluids are not influenced by apparent viscosity under any flow situation. Therefore, characteristics of the Newtonian glycerin solution were observed as apparent viscosity when the Q and ΔP of the other fluid were constant. We also found that a decrease in apparent viscosity may occur upon flow through the oxygenator. When

the flow increased from 2 L/min to 4 L/min, although the estimated viscosity projected constant values, the deemed viscosity projected decreased values. Viscosity of non-Newtonian fluids varies when shear is applied to a fluid. In blood, the apparent viscosity decreases conspicuously until shear rate exceeds 45 s^{-1} , and further increases in shear rate have little effect [36]. Current oxygenators have low shear rates because they are designed for low shear stresses that suppress the activation of blood cells [17]. Therefore, when the flow increased, the deemed viscosity as well as the apparent viscosity likely decreased from the increase in fluidity.

Moreover, the deemed viscosity had a smaller rate of decrease at a high hematocrit level as compared to the estimated viscosity. In narrow tubes carrying red blood cells, the cells gather in the fast-moving center, depending on the heterogeneous distribution, and a plasma layer is formed on the flow path wall [27]. In addition, the erythrocyte distribution is influenced by the hematocrit level at diameters less than $200 \mu\text{m}$ [38]. At high hematocrit levels, the flow path resistance increases because of a thinning plasma layer [28]. Therefore, a sample with a high hematocrit level may have a decrease in apparent viscosity compared with a sample having a low hematocrit level when an average hollow fiber gap of $100 \mu\text{m}$ is available for blood passage. Deemed viscosity was calculated based on resistance parameters derived from the glycerin solution, which is not influenced by shear rates and may behave like apparent viscosity. It should be noted that deemed viscosity can be applied to human blood. Although deemed viscosity cannot estimate the absolute viscosity of blood, it may prove useful in the detection of blockage in an oxygenator flow path, as a relative means of monitoring of the blood viscosity variation of the perfusing oxygenator.

Using the method described here, the input values for viscosity estimation were

limited to flow and inlet/outlet pressure of the oxygenator. Since flow and oxygenator pressure are commonly measured during CPB, this method does not require additional devices. Moreover, more recent HLM can easily acquire these data continuously because the apparatus supports communication ports such as the universal serial bus. Thus, compared to conventional viscosity measurement procedures for sampling blood with the viscometer, this method might provide viscosity measurements through continuous, non-contact monitoring using only the pressure flow information from the oxygenator.

This study has limitations. Since estimated viscosity is measured indirectly based on Q and ΔP , if sudden oxygenator flow pass blockage occurs due to another factor, such as clots and bubbles, this method cannot estimate a correct viscosity value; however, the abnormal estimated value suggests a specific status of the oxygenator while estimated viscosity is evaluated as a relative change. In such clinical incidents, an abnormal value of estimated viscosity may detect failure of the oxygenator rather than the conventional monitoring method based on pressure monitoring alone. Thus, the application of this method during CPB in detection of an oxygenator flow pass blockage with factors such as clots requires further investigation. Since the fluid used in our experiment was bovine blood, there are of course differences in blood cell size and erythrocyte flexibility relative to human blood [39]; therefore, the resistance parameters must be confirmed from pressure flow characteristics using human blood. Additional studies of the accuracy of estimated viscosity using resistance parameters of human blood should also be performed in future. Only one data sample was used for the measurement and estimation of the viscosity; therefore, measurement error due to an unexpected disturbance could occur even under stable conditions. Additionally, only one

experimental system was used throughout this experiment. Hence, there could be different pressure characteristics due to manufacturer variability. The precision and accuracy of the measured viscosity using multiple data samples as well as the manufacturer variability of the oxygenators must be further investigated.

3.6 Conclusion remark

A new method for the estimation of viscosity using Q , P_{in} , and P_{out} was proposed based on a model of pressure and flow in an oxygenator. By conducting systematic experiments with varying hematocrit and temperature levels in bovine blood, we found that η_e correlated with η with good accuracy. Furthermore, we have proposed the blood viscosity monitoring method using glycerin parameters for ease of parameter derivation and evaluated validity of deemed viscosity using bovine blood at different levels of hematocrit, flow, and temperature. The deemed viscosity decreased when compared with measured viscosity, but the relative change corresponded with the temperature change. As hematocrit and flow levels change, because deemed viscosity behaves like apparent viscosity, blood denaturation or initial clots in the perfusing oxygenator may be sensitively detected by changes of the deemed viscosity. Application of this method to obtain continuous estimates of blood viscosity during CPB may be helpful for clinical perfusion management.

Chapter 4

A continuous blood viscosity monitoring system for cardiopulmonary bypass applications

4.1 Introduction

A novel equation to estimate viscosity was proposed based on its pressure flow characteristics in Chapter 3. The hematocrit and temperature were systematically adjusted in *in vitro* experiments using bovine blood and used to evaluate our proposed viscosity estimation method. The estimated viscosity and the measured viscosity were very strongly correlated in all samples. However, because the fluid used for the experiment in Chapter 3 was bovine blood, there are differences in blood cell size relative to human blood. Therefore, the evaluation in the human blood needed to be investigated.

The initial values of the hematocrit levels of patients are different, and the hematocrit level diluted by the physique of the patients is also different. During CPB, hematocrit and the temperature change during a procedure of the surgery. Therefore, in this chapter, we develop a continuous blood viscosity monitoring system based on the methods we previously proposed and apply the continuous monitoring system to clinical cases. Here, we investigated the clinical application of this method by comparing the measured viscosity with the estimated viscosity from clinical cases. In addition, the time-continuous estimation accuracy of the proposed method was evaluated and the technical problems regarding continuous measurements and viscosity calculations were

investigated.

4.2 Continuous blood viscosity monitoring system

The proposed system consists of three parts as shown in Fig. 4.1:

- 1) Signal measurement comprising CPB circuits and the HLM;
- 2) Blood viscosity estimation; and
- 3) Display on a computer screen.

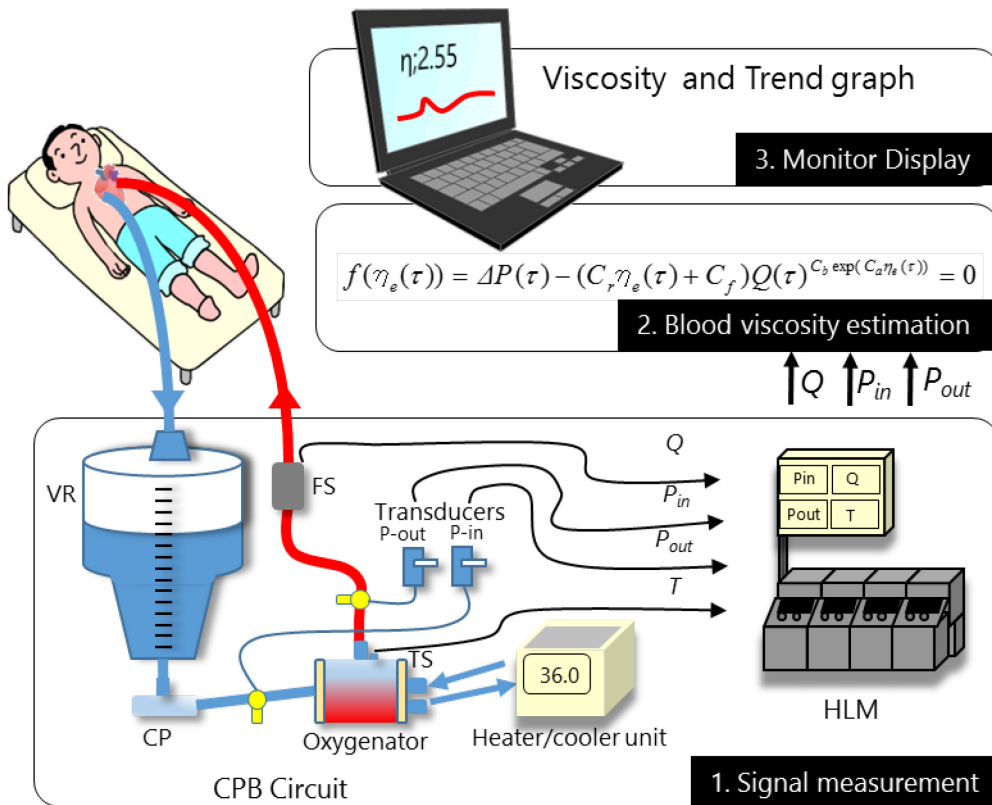


Fig. 4.1 Overview of the CPB circuit and system. CP: centrifugal pump; FS: flow sensor; HLM: heart lung machine; P_{in} : inlet pressure; P_{out} : outlet pressure; Q : blood flow; T : Temperature; TS: Thermal sensor; and VR: venous reservoir.

4.2.1 Signal measurement

The signal measurement component measures inlet pressure (P_{in}), outlet pressure (P_{out}), and blood flow (Q) from the oxygenator, all of which are required to estimate blood viscosity (η_e). Because these quantities are routinely measured for perfusion management during CPB and are monitored on the HLM, the values are available for any type of CPB circuit, such as open-type and close-type. For example, P_{in} and P_{out} are generally measured by liquid seal-type pressure transducers attached to the oxygenator's inlet and outlet tubes. In addition, Q is measured by a flowmeter using ultrasound technology in the case that a centrifugal pump is used as a blood pump, and in the case of a roller pump, Q is measured on the HLM from the pump tube size and the number of rotations for a particular pump occlusion setting. It should be noted that measurement accuracy of the devices used for measurement may affect accuracy of the estimated viscosity.

As mentioned above, the measured P_{in} , P_{out} , and Q values are accumulated in the HLM and monitored. Most current HLMs are equipped with a Universal Serial Bus (USB) interface. In this study, the HLM model number HAS-2 (Senko Medical Instrument Mfg. Co., Ltd., Tokyo, Japan) is used, and it is provided with a USB interface, including a USB port that enables communication between HAS-2 and a computer. The USB interface communicates with the computer using the control transfer protocol, and it can output data every 0.5 s upon request from the computer. The communication program between HAS-2 and the computer was created using Microsoft Visual C++ 2013 and WinUSB driver.

4.2.2 Blood viscosity estimation

For the blood viscosity estimation, η_e is calculated from the oxygenator pressure gradient ($\Delta P = P_{in} - P_{out}$) and Q acquired from the HLM. In Chapter 3, we have documented that η_e can be modeled as a function of ΔP and Q by the following relational expression, in which τ is the sampling time.

$$f(\eta_e(\tau)) = \Delta P(\tau) - (C_r \eta_e(\tau) + C_f) Q(\tau) C_b \exp(C_a \eta_e(\tau)) = 0. \quad (4.1)$$

Provided with the resistance parameter set determined for any given oxygenator and fluid, $\eta_e(\tau)$ can be estimated from $P_{in}(\tau)$, $P_{out}(\tau)$, and $Q(\tau)$.

Evaluating the reliability of η_e is important for real-time continuous monitoring in clinical applications. In the previously proposed method, $\eta_e(\tau)$ was estimated using measurement data at a single sampling point, which can be vulnerable to noise contamination. Therefore we assumed that the time-variation of the blood viscosity is small, and estimated $\eta_e(\tau)$ using data in a window width of N samples, which is conducted by minimizing the evaluation function given by Eq. (4.2) using the Levenberg-Marquardt method, where $\Delta P(\tau - i)$ is the pressure gradient of the oxygenator measured at i sampling time before the present sampling time τ . The computer program used in this blood viscosity estimation component was created using Microsoft Visual C++ 2013.

$$J(\tau) = \sum_{i=0}^N \Delta P(\tau - i) - (C_r \eta_e(\tau) + C_f) Q(\tau - i) C_b \exp(C_a \eta_e(\tau)). \quad (4.2)$$

4.2.3 Display

Fig. 4.2 shows the control panel and monitoring screen of the proposed system. This control panel allows parameters to be manually set, which corresponds to selecting oxygenator and fluid types. Four buttons aligned on the top row of the control panel enable commands to be sent through the established USB connection to initiate and terminate viscosity monitoring, as well as review the recorded data. With this control panel, one can start monitoring and recording the data within two clicks of a mouse, so that there is very little burden on the perfusionist to operate the system. The monitoring panel displays estimated viscosity η_e in real time. The left three graphs show the most recent 1200 s of data for η_e , ΔP , and Q , and the right three graphs show the data over the whole measurement period. Showing recent data trends facilitates detecting blockage of the oxygenator flow path during CPB because Fisher *et al.* reported that the blockage causes abnormal changes in the pressure gradient ΔP over approximately 1200 s [21]. The data from the whole measurement period then helps the perfusionist evaluate continuous variation from the initiation of CPB.

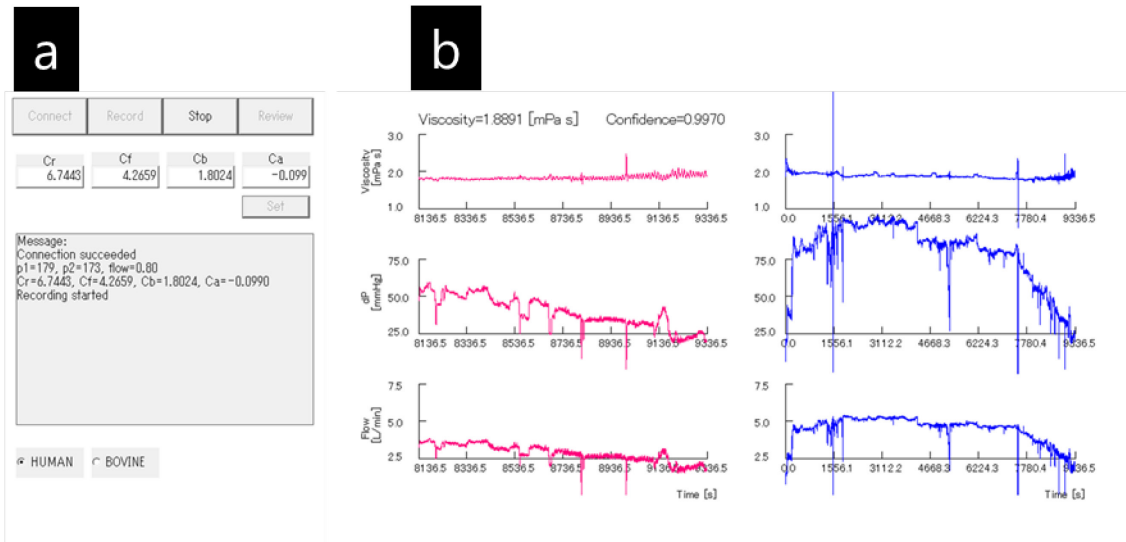


Fig. 4.2 Continuous blood viscosity monitoring system display, with two windows: (a) control panel, in which the upper buttons allow selection of oxygenator and initiation and termination of estimated viscosity monitoring, and (b) monitoring screen, where real-time η_e is displayed at top, trends in η_e , ΔP , and Q over the whole measurement period are displayed in the graphs on the right, and the graphs on the left show the same parameters over the most recent 1200 s.

4.3 Materials and methods

This section describes the experimental procedures for deriving the human blood resistance parameters and for comparing the measured blood viscosity (η) with the estimated blood viscosity (η_e). Furthermore, the proposed real-time monitoring system was applied to clinical cases and the precision of η_e was evaluated. Studies on human subjects were performed according to the principles of the Declaration of Helsinki. All procedures of this study were approved by the Ethical Committee of Hiroshima University (1172). All data are presented as the mean \pm the standard deviation. Statistical analysis was performed using XLSTAT software and JMP 11.0 (SAS Institute Japan Ltd., Tokyo, Japan) for *t*-test, regression analysis, and Bland-Altman plotting. Statistical significance was assumed when $p < 0.05$.

4.3.1 Experimental determination of human blood resistance parameters

The human blood resistance parameters were derived by the following experiments. A membrane oxygenator with a 32 μm integrated artery filter (CAPIOX-FX15; from Terumo Cardiovascular Systems Corp., Tokyo, Japan) and an average hollow-fiber gap of 100 μm was used for the passage of blood. The oxygenator's purge line was closed during the experiment. The oxygenator and venous reservoir (CX-RR40; Terumo Cardiovascular Systems Corp.) and centrifugal pump (MP-23; Senko Medical Instrument Mfg. Co., Ltd.) were connected with 3/8 inch polyvinyl chloride tubing to form a closed circuit; these components comprised the *in vitro* experimental system as shown in Fig. 2.1.

A three-way stopcock was attached to an inlet tube and the oxygenator outlet, and pressure was measured from the stopcock through a transducer (DTCL03; Argon Medical Devices Japan, Inc., Tokyo, Japan: measurement accuracy is $\pm 3\%$). An ultrasonic blood flowmeter (Transonic H9XL; Transonic Systems Inc., Ithaca, NY, USA: measurement accuracy is $\pm 10\%$) was installed on the exit-side tube of the oxygenator. A heat exchanger was connected to the oxygenator, and the temperature was measured at the oxygenator outlet. The inlet and outlet pressures, flow, and temperature of the oxygenator were displayed on an artificial HLM (HAS-2; Senko Medical Instrument Mfg. Co., Ltd.).

Expired, irradiated, concentrated, leukocyte-reduced RBCs without plasma (Japanese Red Cross Society, Tokyo, Japan) were accumulated in the venous reservoir with Albuminar-5 (CSL Behring K.K., Tokyo, Japan) and 0.9% saline. When the oxygenator outlet temperature of the samples perfused through the test circuit became stable at 36 °C, then 3 mL of the sample was obtained from the circuit, and η and hematocrit were measured using a torsional oscillation viscometer (VISCOMATE VM-10A; Sekonic Co. Ltd., Tokyo, Japan), and a complete blood count was taken (MEK-6500; Nihon Kohden Co., Ltd., Tokyo, Japan). The sample was immediately placed into a sample cup and measured under static conditions. The temperature was monitored during each η measurement by means of sample cups placed in a water bath equilibrated to the temperature at 36 °C, and η was recorded 10 seconds after the start of the measurement. Samples with viscosities of 1.88, 2.33, and 2.80 mPas were prepared by hemoconcentration using a blood concentrator and dilution with 0.9% saline; hematocrits were 14.1%, 24.5%, and 30.7% RBC, respectively. Each sample was perfused and circulated through the test circuit at a constant temperature of 36 °C. The

rotational speed of the centrifugal pump was increased from 1,000 to 3,500 rpm in 100 rpm intervals at approximately every 3 minutes after each data recording. The mean P_{in} and P_{out} of the oxygenator and Q of each rotational speed were recorded. ΔP and Q were plotted, and an exponential power was derived to approximate a relational expression for ΔP and Q in each sample.

Using the obtained results, the human blood resistance parameter set was determined using the method described in Chapter 3. This parameter set was inputted to the proposed system through the display's control panel, and viscosity was estimated using Eq. (4.2). Using this experimental data, we compared a linear approximation curve obtained from the conventional method [16] with the exponential approximation curve obtained by the proposed method, and we investigated the significance of the curve fitting. A statistic comparison between the linearity of the conventional method and the nonlinearity of the proposed method was performed by calculating the sum of squared residuals of each curve fitting, and the sum of squared residuals was then examined for each sample by a t -test.

4.3.2 Accuracy of estimated viscosity

During the period of 9 months, 20 patients ($n = 20$) with valvular heart disease underwent elective cardiac surgery with CPB at Hiroshima University Hospital; certain patient characteristics are presented in Table 4.1. The same CPB circuit and procedures, including cardioplegia and anesthesia management, were applied for all patients. The perfusion management was operated at a temperature of 34 °C during aortic cross-clamping, and the hematocrit level was maintained at more than 21%, with a perfusion rate of 2.5 L/min/m². The oxygenator (CAPIOX-FX15; Terumo

Cardiovascular Systems Corp.), a venous reservoir (CX-RR40; Terumo Cardiovascular Systems Corp.), and a centrifugal pump (MP-23; Senko Medical Instrument Mfg. Co., Ltd.) were connected with 3/8 inch polyvinyl chloride tubing to form a standard opened circuit; these components comprised the clinical system, as shown in Fig. 4.1. The oxygenator's purge line was closed during CPB following the recommendation of the manufacturer of the FX15 oxygenator. A three-way stopcock was attached to an inlet tube and the oxygenator outlet, and pressure was measured from the stopcock by a transducer (DTCL03; Argon Medical Devices Japan, Inc.). An ultrasonic blood flowmeter (Transonic H9XL; Transonic Systems, Inc.) was installed on the tube exiting the oxygenator. A heat exchanger was connected to the oxygenator, and the temperature was measured at the oxygenator outlet. The inlet and outlet pressures, Q , and temperature of the oxygenator were output through the HLM's USB port (HAS-2; Senko Medical Instrument Mfg. Co., Ltd.). The system that estimates viscosity using Eq. (4.2) from the measured P_{in} , P_{out} , and Q was also connected to the HLM by the USB interface.

Table 4.1 Patient characteristics

AVR : MVR	13 : 7
Male : Female	11 : 9
Age (years)	72.6±10.9
BSA (m ²)	1.56±0.16
ECC (min)	165.4±47.8
ACC (min)	94.3±35.9
Minimum BT (°C)	33.7±1.54
Pre-hematocrit (%)	33.0±4.4

AVR: Aortic valve replacement; MVR: Mitral valve replacement; ECC: Extracorporeal circulation time; ACC: aortic cross-clamp time; BSA: Body surface area; BT: Blood temperature. Pre-hematocrit is defined as the hematocrit value just before the initiation of CPB.

Table 4.2 Patient characteristics

AVR : MVR	7 : 3
Male : Female	4 : 6
Age (years)	69.9±12.2
BSA (m ²)	1.57±0.19
ECC (min)	179.8±83.0
ACC (min)	106.3±50.9
Minimum BT (°C)	32.5±1.0
Pre-hematocrit (%)	33.9±4.7

AVR: Aortic valve replacement; MVR: Mitral valve replacement; ECC: Extracorporeal circulation time; ACC: aortic cross-clamp time; BSA: Body surface area; BT: Blood temperature. Pre-hematocrit is defined as the hematocrit value just before the initiation of CPB.

After initiating CPB, η_e and the temperature were recorded over three periods, which were chosen to represent the three thermal phases in CPB (i.e., before cooling, during stable hypothermia and after rewarming): after establishing total CPB, after the aortic cross-clamp, and after declamping. At the same time, blood samples were collected from the circuit and hematocrit, η was measured using a torsional oscillation viscometer (VISCOMATE VM-10A; Sekonic Co. Ltd.), and a complete blood count was taken (MEK-6500; Nihon Kohden Co., Ltd.). Because continuous measurement of η by a torsion oscillation viscometer is impossible, η_e was calculated using the single point obtained at the time the blood sample was collected, with the window width $N = 1$. The measured values for η , hematocrit, and temperature after establishing total CPB were compared to the corresponding values for the other two phases to evaluate the influence of event change during CPB. The estimated η_e was plotted as a function of η , and the systematic errors and compatibility between the estimated and measured values were assessed by Bland-Altman analysis, as presented in Section 4.4.

4.3.3 Robustness improvement following clinical applications

During a period of 4 months, 10 patients ($n = 10$) with valvular heart disease underwent elective cardiac surgery with CPB at Hiroshima University Hospital; certain patient characteristics are presented in Table 4.2. The same CPB procedures, including cardioplegia and anesthesia management, were applied to all patients, and the CPB system described in Section 4.3.2 was used. A blood parameter monitoring system (CDI-500; Terumo Cardiovascular Systems Corp.) was used in all cases for the continuous measurement of hematocrit; calibration was conducted within 5 minutes after initiating CPB, and recalibration was performed at each interval of 30 minutes

During CPB, η_e , ΔP , Q , and temperatures of all patients were recorded by this system. To guarantee the accuracy of continuously estimated viscosity, countermeasures for noise contamination during CPB are required. Therefore, we defined a reliability index $\varepsilon(\tau)$ given by Eq. (4.3) to evaluate the estimated data. The reliability index is displayed together with the estimated viscosity for verification of measured pressures and blood flow on the monitoring panel.

$$\varepsilon(\tau) = \frac{\sum_{i=0}^N \Delta P(\tau - i)^2}{\sum_{i=0}^N \Delta P(\tau - i)^2 + \sum_{i=0}^N \left(\Delta P(\tau - i) - \Delta \hat{P}(\tau - i) \right)^2}. \quad (4.3)$$

$\Delta \hat{P}(\tau - i)$ is the estimated pressure gradient of the oxygenator determined by substituting $\eta_e(\tau - i)$ in Eq. (4.1).

To improve the robustness of the real-time estimation of η_e , the proposed method's accuracy was evaluated by adding white Gaussian noise to all measured samples of ΔP . For this purpose, we denote $\Delta P_\sigma(\tau)$ as the pressure gradient with white Gaussian noise generated from $N(0, \sigma^2)$ added. The blood viscosity $\eta_{e,\sigma}(\tau)$ was estimated using Eq. (4.2), substituting $\Delta P_\sigma(\tau)$ for $\Delta P(\tau)$. Subsequently, $\Delta \hat{P}_\sigma(\tau)$ was calculated by substituting the estimated $\eta_{e,\sigma}(\tau)$ in Eq. (4.1). Finally, the reliability index was derived using Eq. (4.3), where $\varepsilon(\tau) = \varepsilon_\sigma(\tau)$ and $\Delta \hat{P}(\tau - i) = \Delta \hat{P}_\sigma(\tau - i)$. In this evaluation, the reliability index $\varepsilon_\sigma(\tau)$ was calculated for different window widths N in ranges [1, 50] and different standard deviations of white Gaussian noise σ in ranges [1, 20]; the Bayesian Information Criterion (BIC) was used to determine the optimal window width N at which $\varepsilon_\sigma(\tau)$ approximates 1. It should be noted that $N = 1$ is equivalent to the previously proposed method.

To discuss the estimation accuracy, first, we show the trends of η_e estimated using the optimal window width N as well as ΔP and Q from the initiation of CPB for one subject. Please note that this phase just after the initiation of CPB generally yields noisy data because blood flow changes most. Subsequently, for each clinical case, the average determination coefficients and their standard deviations were respectively calculated between η_e and the hematocrit and temperature parameters measured at intervals of 6 s. In addition, the distribution of η_e over the whole CPB period was analyzed by a histogram with a bin size of 0.05 mPas.

4.4 Results

4.4.1 Resistance parameters of human blood

Fig. 4.3 shows pressure-flow characteristics of human RBC suspensions. Both the exponential and linear approximations of ΔP relative to Q showed very high determination coefficients. The human RBC resistance parameters for the FX15 oxygenator were derived from the exponential approximation curve, as presented in Table 4.3.

The coefficients determined by the exponential approximation were 0.9992 at 1.88 mPas, 0.9989 at 2.33 mPas, and 0.9998 at 2.80 mPas. The coefficients determined by the linear approximation were 0.9891 at 1.88 mPas, 0.9935 at 2.33 mPas, and 0.9945 at 2.80 mPas. In all samples, the sum of squared residuals between the two curve fittings confirmed the significant differences, with $p < 0.001$.

Table 4.3 Coefficients for Human RBC Suspensions

Resistance parameters	C_r	C_f	C_b	C_a
RBC suspensions	6.7443	-4.2659	1.8024	-0.099

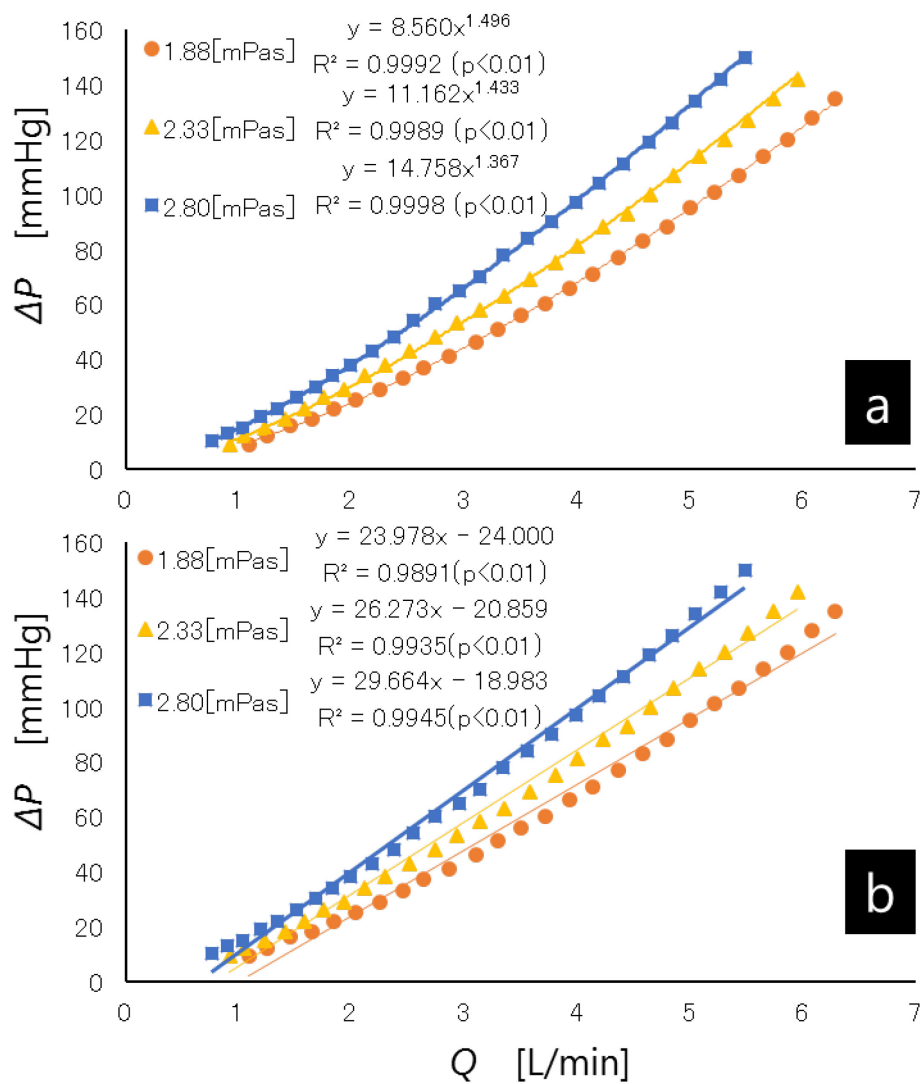


Fig. 4.3 Pressure gradient ΔP relative to flow Q for a human RBC suspension fitted to two different curves: (a) exponential approximation and (b) linear approximation.

4.4.2 Correlation between measured and estimated viscosity and Bland-Altman analysis

The comparison of η_e and η is shown in Fig. 4.4. The parameters η_e and η showed a very strong correlation, with $R^2 = 0.9537$, and $p < 0.001$. Fig. 4.5 shows a plot of the Bland-Altman analysis, which revealed a mean bias of -0.002 mPas, a standard deviation of 0.03 mPas, limits of agreement of -0.06 mPas to 0.07 mPas, and 3.4% error. There was no fixed or proportion bias ($R^2 = 0.063$, $p > 0.05$) for the viscosity.

Fig. 4.6 shows the relative η_e , hematocrit, and temperature at three different phases ($n = 20$); η_e was 1.92 ± 0.12 mPas after establishing total CPB, 1.96 ± 0.14 mPas after aortic cross-clamp, and 1.90 ± 0.15 mPas after declamping. Hematocrit levels were $22.9 \pm 3.1\%$ after establishing total CPB, $23.7 \pm 2.7\%$ after aortic cross-clamp, and $23.9 \pm 2.1\%$ after declamping. The temperatures were 35.0 ± 0.7 °C after establishing total CPB, 33.0 ± 1.6 °C after aortic cross-clamp, and 36.6 ± 0.8 °C after declamping. Compared to the phase after CPB has been established, there were no significant differences between the other two phases in η and hematocrit. As for the temperatures, the significant difference was also found between the first phase against the other two phases, which exhibited $p < 0.01$ relative to each other.

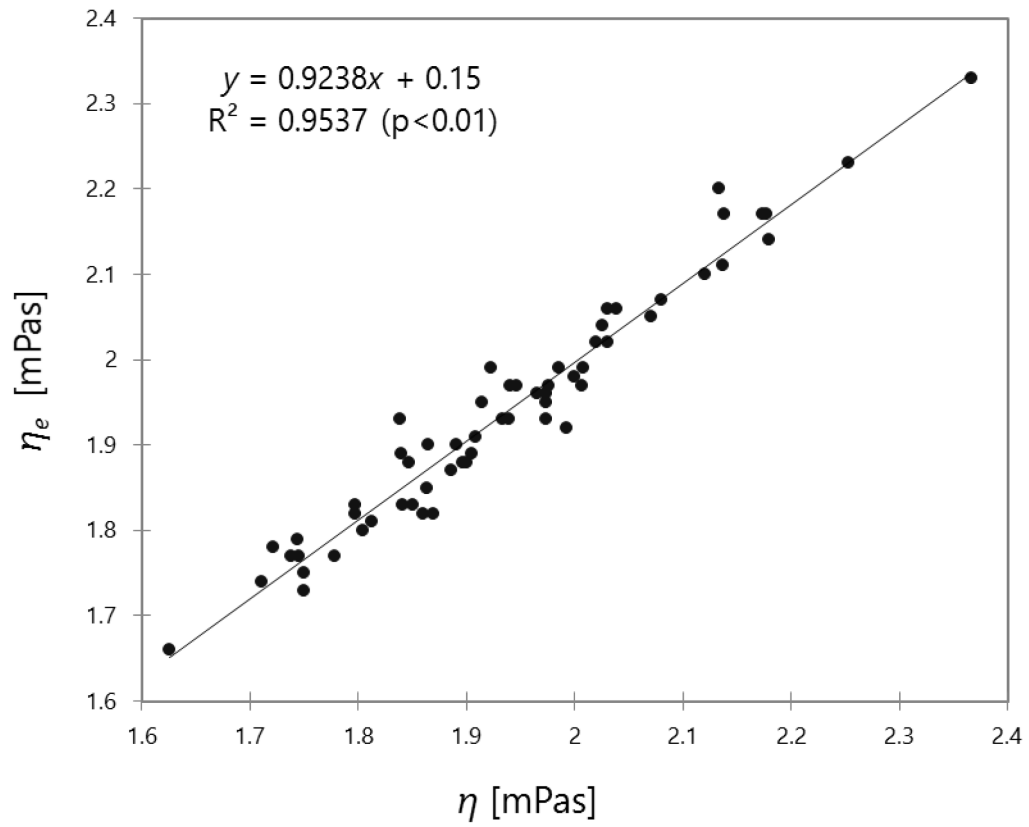


Fig. 4.4 Correlations between and linear regression analysis of the equation used to estimate viscosity η_e and viscosity measured with a VM10-A viscometer η .

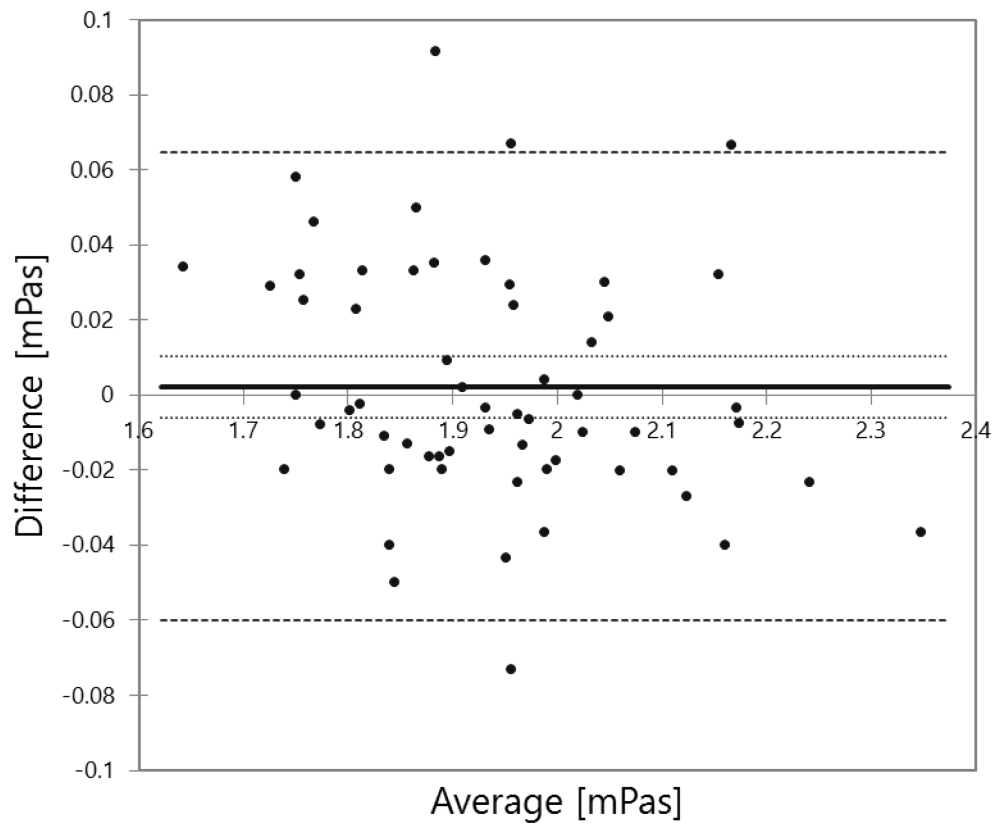


Fig. 4.5 Bland-Altman plot comparing estimated and measured viscosity. The solid line denotes bias (mean of difference), the large dashed line denotes the 95% limits of agreement (two standard deviations of difference), and the small dashed lines denote the 95% confidence interval for the difference between the means.

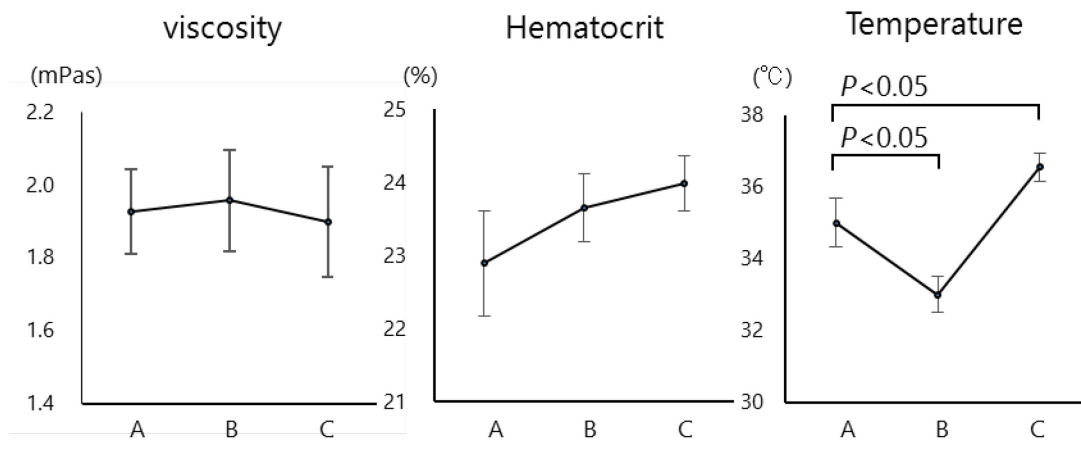


Fig. 4.6 Results of mean value changes in estimated viscosity, hematocrit, and temperature at three points: A, after total CPB has been established; B, after aortic cross-clamp; and C, after declamping.

4.4.3 Optimal window for the algorithm based on clinical applications

Fig. 4.7 shows the window width N against the reliability index $\bar{\varepsilon}_\sigma$, representing the average of $\varepsilon_\sigma(\tau)$ over time, when the white Gaussian noise of different standard deviations was applied. A small window width N exhibited low precision if noise was increased; in contrast, a plateau trend was observed as window width N increased. This is because the estimated η_e is vulnerable to noise if N is small; however, with a large N , η_e can lose its dynamic sensitivity. According to BIC, the optimal window width N was 8. Fig. 4.8 shows the graph of η_e estimated by window width $N = 8$, as well as ΔP and Q , from initiation of CPB to 100 s after the initiation.

Fig. 4.9(a) shows the relationship between η_e and hematocrit. The mean determination coefficient for all cases, showed a weak correlation at 0.33 ± 0.14 . Fig. 4.9(b) shows the relationship between η_e and temperature. The mean determination coefficient for all cases was 0.22 ± 0.21 . Fig. 4.10 shows a histogram of η_e for all cases, illustrating that 98% of estimated viscosity η_e was distributed in a range of 1-3 mPas.

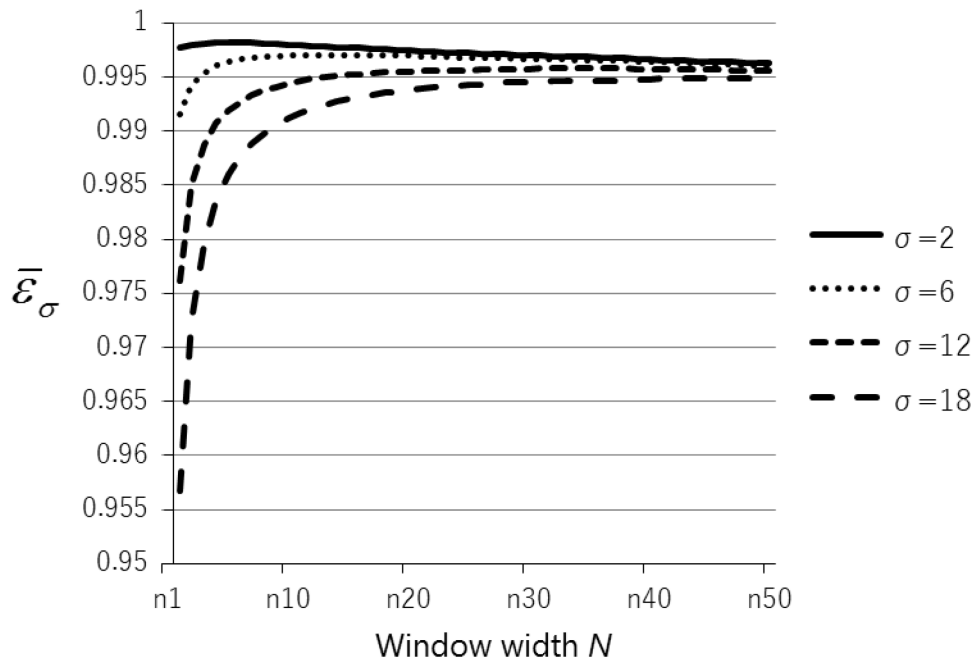


Fig. 4.7 Relationship between reliability index $\varepsilon_\sigma(\tau)$ averaged over time $\bar{\varepsilon}_\sigma$ and window width N when white Gaussian noise of different standard deviations σ was added to ΔP .

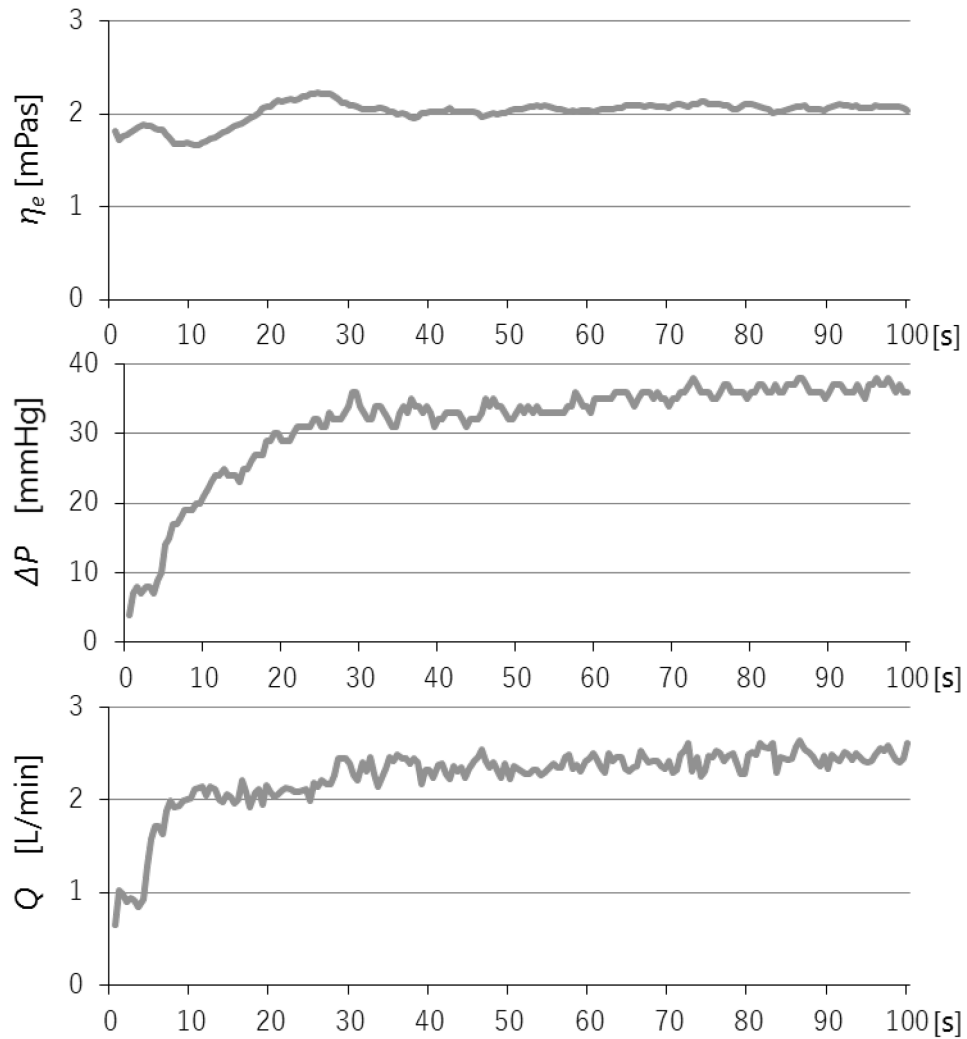


Fig. 4.8 Sample of monitored data during 100 s after initiation of CPB. The graphs show η_e estimated using window width $N = 8$, and ΔP and Q measured from one subject. After initiation of CPB, ΔP increases with increased Q . Although η_e was initially a low value because of dilution with the priming solution, the blood and priming solution mixed 30 s later and were stable. Although estimated η_e showed an almost stable tendency, ΔP and Q were unstable, with amplitudes of approximately ± 5 mmHg and ± 0.5 L/min, respectively.

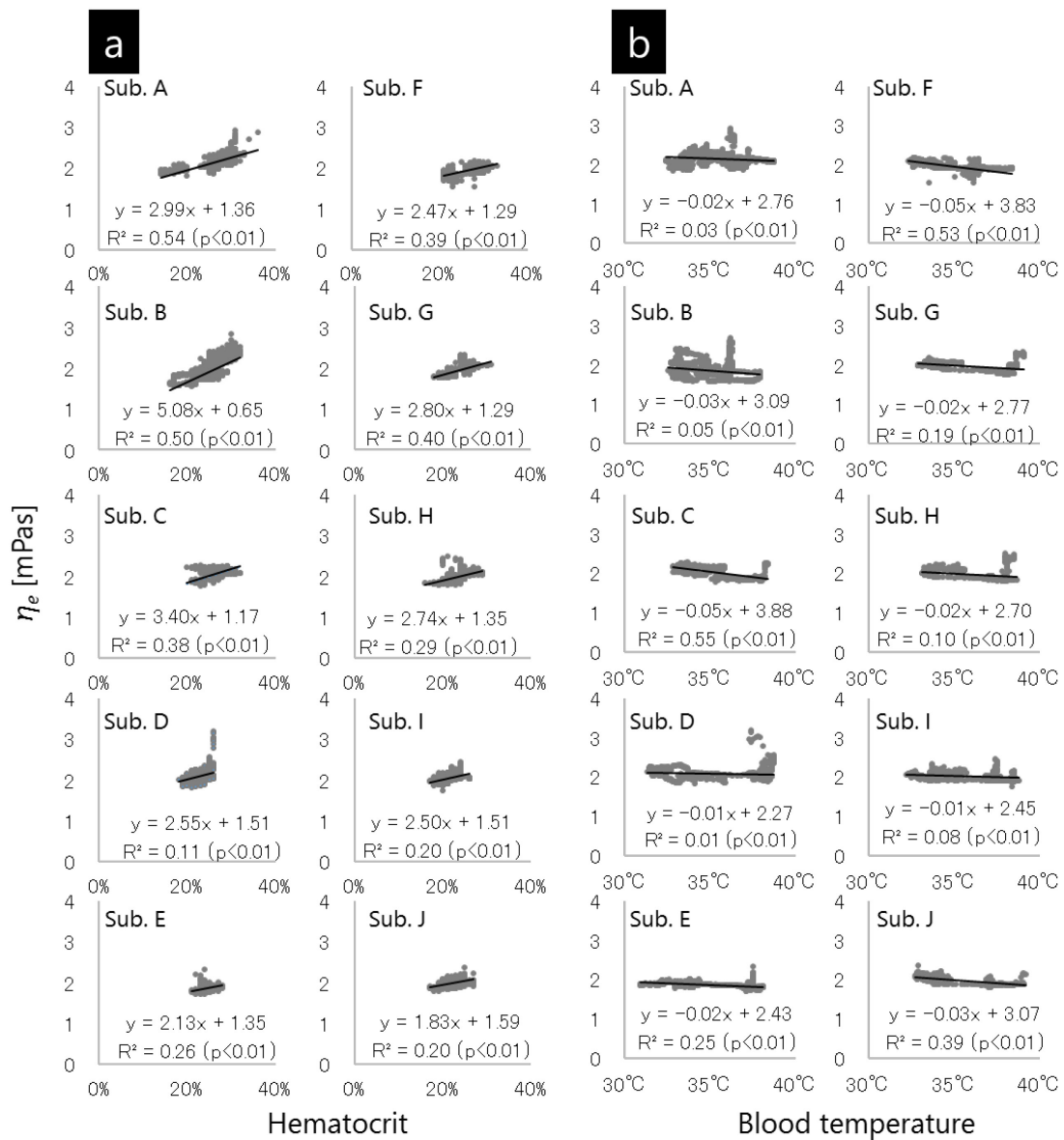


Fig. 4.9 (a) Correlation between and linear regression analysis of estimated viscosity η_e and measured hematocrit. (b) Correlation between and linear regression analysis of estimated viscosity η_e and measured blood temperature.

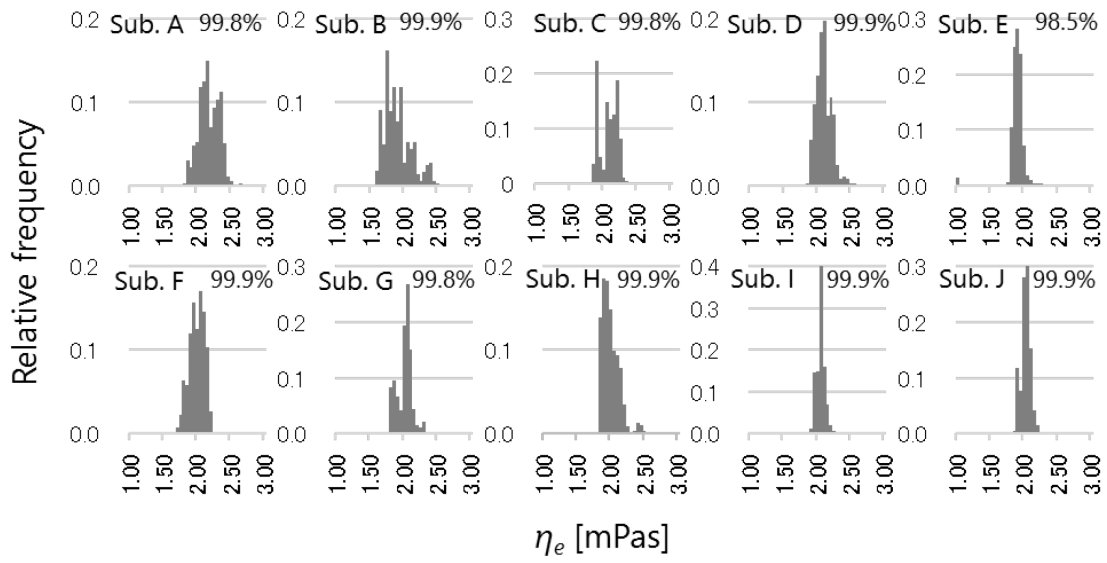


Fig. 4.10 Histogram of η_e with bin size of 0.05 mPas; each graph shows a relative frequency for all measurement points, and the percentage value attached on each histogram is the occurrence ratio of data in the range of 1–3 mPas among all values.

4.5 Discussion

The proposed method is based on the pressure-flow characteristics of the fluid perfusing through the oxygenator. We compared the curve fitting accuracies of the linear curve based on Poiseuille's law and the proposed exponential curve, and investigated an optimal model. Although both models yield excellent fittings in terms of the determined coefficients, the proposed exponential model was significantly better than the linear model with respect to the fitting error. Therefore, the proposed exponential model was employed to model pressure-flow characteristics, and four resistance parameters were determined.

The viscosity estimated using the proposed method was compared to the viscosity measured using a viscometer at three main events during CPB. The continuous blood viscosity monitoring system was developed based on the algorithm described above for the estimation of viscosity. The accuracy of the estimation can be low in cases where a large measurement noise is continuously mixed into ΔP and Q , which can happen during the period after initiation of CPB. In addition, an instantaneous noise introduced to the pressure measurement can be caused by operation procedures and errors, such as aortic cross-clamp and blood drainage failure, after the establishment of total CPB [40]. Therefore, to achieve robustness for precise continuous monitoring, the estimation algorithm should minimize these influences. We thus investigated the optimal window width N from the data obtained by applying this system to clinical CPB cases.

Furthermore, through two experiments in clinical cases, we obtained some findings about the relationships between blood viscosity and hematocrit, and between blood viscosity and temperature, during CPB. The blood viscosity measured at establishment of total CPB was compared to the other two phases during CPB; in this first phase, the

blood was diluted most. Viscosity increased after aortic cross-clamp, which had the lowest temperature, and viscosity decreased after declamping, which had the highest temperature. However, there was no significant difference in blood viscosity levels because hematocrit levels were controlled by transfusion and hemoconcentration so that the hematocrit level was never lower than 21%. In this study, there were no abnormal blood viscosity measurements in any phase of any case. The η_e recorded continuously for all periods during CPB was compared with hematocrit and temperature. During CPB, although changes in viscosity are primarily due to changes in hematocrit levels and blood temperature, there was only a weak correlation between η_e and hematocrit. In addition, although the patient characteristics varied before initiating CPB, with BSA at 1.31–1.81 m² and hematocrit levels at 26.7–40.5%, η_e was concentrated in a range from 1.5 to 2.5 mPas for all cases. Because blood viscosity during CPB showed a tendency to be distributed over a constant range without relation to BSA and hematocrit levels, in the situations where viscosity exceeds 3.0 mPas, careful monitoring is necessary. It should be noted that addition of 1,000 mL infusion solution due to anesthesia introduction and hemorrhage by operation procedures before CPB induction may be more influential on low pre-hematocrit level of the subjects, who consist of aged Japanese persons whose physique is generally smaller in comparison with Westerners. However, accumulation of further data is necessary because we consider it more relevant to focus on a relative change in blood viscosity rather than its absolute value.

Because the minimum average blood temperature of the subjects was 32.5 °C, blood viscosity may have not been affected. In chapter 3, in which bovine blood at hematocrit 21.8% was used, we confirmed a viscosity change of approximately 10% during a temperature change from 37 to 31 °C. This is consistent with the results using the

human blood reported by Eckmann [36]. As for mild hypothermic CPB, the influence of blood viscosity was slight; depending on controlled hematocrit levels during CPB, it was thought that blood viscosity was stable. However, abnormal blood viscosity during CPB may not be explained solely from changes in temperature and hematocrit levels because influences on blood viscosity during CPB are multifactorial. The patients with cold agglutinins may experience RBC agglutination due to steep declines in blood temperature [23], whereas blood is exposed to non-physiological, mechanical stress during CPB. Extreme pH changes in blood may also affect RBC shape, which can in turn impair tissue perfusion [24]. In addition, because blood transitions from a liquid to a gel phase during coagulation [22], in cases of insufficient anticoagulation, an increase in blood viscosity may stop oxygenator flow because of clot formation. Therefore, although blood viscosity did not show abnormal values in these clinical cases, it must be monitored carefully during CPB because abnormal blood viscosity may affect the perfusion.

Using the proposed method, the input values for the viscosity estimation were limited to flow and the oxygenator's inlet and outlet pressures. Because flow and pressures are commonly measured during CPB [41], this method does not require additional devices. Moreover, the HLM can easily acquire these data continuously because the apparatus supports communication ports, such as USB. The system proposed here allows communication with the HLM by the USB interface and does not require complicated maneuvers on the part of the user. This system may be even more beneficial to patients undergoing extracorporeal membrane oxygenation (ECMO). ECMO is a technique in which the oxygenator provides cardiopulmonary support to patients with severe refractory cardiac and respiratory failure; however, the reported rate of neurologic

complications is between 4–11% [42]. Future research should apply the proposed technology to investigate viscosity changes independent of temperature (e.g., hyperviscosity due to insufficient anticoagulation and hypoviscosity due to hypoproteinemia) during ECMO. This study validates the application of the proposed continuous blood viscosity monitoring system during CPB. In future studies, this new method for estimating viscosity should be useful for detecting various viscosity-related effects that may occur during CPB.

This study has several limitations. First of all, it is known that the blood-material interaction in an oxygenator results in protein absorption [43], and this biofouling can become so significant that it decreases the void fraction of the oxygenator fibers and thus increases the pressure gradient over the oxygenator. Because blood viscosity in the proposed algorithm is derived only from blood flow and pressure gradient, it is very difficult to distinguish if the predicted increase in viscosity is a result of real increase in viscosity or a result of biofouling that narrows the passage. This is a limitation of the proposed method. Although blood viscosity variation is influenced by shear rate, the shear rate in a perfusing oxygenator was not examined. An additional study on the effect of shear rate variation on blood viscosity during CPB should be performed in future. Furthermore, because the parameters for the experiments were derived for a closed oxygenator purge line, the application of the proposed method in cases of an opened purge line was not demonstrated. While the oxygenator purge line can be opened to eliminate gaseous microemboli, the opened purge line can change some flow and pressure values [44], which can cause an error factor impacting the estimated viscosity. Further investigations should determine the correct parameters for the opened purge line and how these parameters influence the estimation accuracy.

Clinical trials of this study did not investigate thoracic aortic disease and ischemic heart disease, which have specific impacts on varying blood viscosity. Deep hypothermia circulatory arrest procedures used during thoracic aortic surgery considerably decrease blood temperature as the body temperature is lowered to < 20 °C. It is known that coronary artery bypass grafting (CABG) patients have on average a higher fibrinogen levels [45], a major determinant of plasma viscosity. Therefore, the application of this method in temperature ranges seen during deep hypothermia CPB and CABG procedures must be investigated. In addition to the limitations associated with the observational design of this study, we did not examine postoperative neurologic complications including impaired consciousness, seizures, cognitive impairment, and stroke, which may provide valuable information for improving perfusion management of CPB patients. Furthermore, the small study size of 10 to 20 patients is also a limitation. Therefore, additional investigations of the role of blood viscosity information are required for management of CPB procedures using this technology.

4.6 Conclusion remark

This chapter presented the development and evaluation of an algorithm for a continuous blood viscosity monitoring system and its clinical application. First, we demonstrated that the curve fitting of the proposed algorithm was more appropriate than the conventional model. Second, a strong correlation and good accuracy were found between the viscosity estimated by the proposed method and the viscosity measured using the torsional oscillation viscometer. Last, we applied this system to clinical CPB cases and achieved robustness improvement. These results warrant further investigation into the accumulation and analysis of blood viscosity data during CPB using this

system.

Chapter 5

Conclusions

This dissertation proposed a novel blood viscosity estimation method during CPB based on the idea of estimating viscosity from the pressure-flow characteristics model of an oxygenator. The derivation of a pressure-flow characteristics model using the parameters in three different fluids, the proposal of a viscosity estimation algorithm using the model, and a demonstration of accuracy between the proposed method and the conventional method using viscometer were described. A proposed method for clinical application to a continuous blood viscosity monitoring system developed was also outlined. As this method can acquire blood viscosity information by using a simple, continuous, non-contact monitoring system, evaluating influences on blood viscosity during CPB may result in improvement of perfusion management.

Chapter 2 described the modeling of pressure-flow characteristics of an external perfusion-type oxygenator and the derivation of parameters for three different fluids: a glycerin solution modeled as a Newtonian fluid; and whole bovine blood and human RBC suspensions, both modeled as non-Newtonian fluids. The author uses the results to quantify how viscosity is affected by this device. As for the pressure-flow characteristics obtained for three viscosity levels of each fluid, all samples showed agreement with a coefficient of determination of almost 1 by exponential approximation ($R^2 = 0.99$ $p < 0.001$). These results also showed that this model derived a set of resistance parameters corresponding to the characteristics of the fluids because the pressure-flow characteristics were different depending on the type of fluid.

Chapter 3 proposed a novel equation, based on the pressure-flow characteristics of the oxygenator, which uses inlet pressure, outlet pressure, and blood flow from the oxygenator to estimate the viscosity of the fluid perfusing the oxygenator. Using bovine blood for *in vitro* experiments, the accuracy between the viscosity calculated using the equation and the viscosity measured using a torsional oscillation viscometer were systematically investigated for three hematocrit levels during a temperature change. The results demonstrated a strong correlation ($R^2 = 0.962$, $p < 0.001$) and good accuracy (a mean bias of -0.026 mPas, a standard deviation of 0.071 mPas, limits of agreement of -0.114 mPas to 0.166 mPas) between the measured and estimated viscosities. In addition, the deemed viscosity expressed by method using glycerin parameters for ease of parameter derivation was proposed and compared to the evaluated validity of deemed viscosity using bovine blood at different levels of hematocrit, flow, and temperature. The deemed viscosity decreased when compared with measured viscosity, but the relative change corresponded with the temperature change ($R^2 = 0.913$, $p < 0.001$). As hematocrit and flow levels change, because deemed viscosity behaves like apparent viscosity, blood denaturation or initial clots in the perfusing oxygenator may be sensitively detected by changes in the deemed viscosity.

Chapter 4 describes the application of the continuous blood viscosity monitoring system based on the proposed algorithm to clinical cases. The application of this system to clinical experiments with 20 patients indicated a strong correlation ($R^2 = 0.954$, $p < 0.001$) and good accuracy (a mean bias of -0.002 mPas, a standard deviation of 0.03 mPas, limits of agreement of -0.06 mPas to 0.07 mPas) between the viscosity estimated by the proposed method and the viscosity measured using the torsional oscillation viscometer. Furthermore, this system was applied to 10 patients that resulted in

improvement of robustness of the proposed algorithm from the acquired continuous estimated blood viscosity data. These results warrant further investigation into the accumulation and analysis of blood viscosity data during CPB using this system.

Finally, a number of issues to be addressed in future research should be discussed. The proposed method has been successfully applied to clinical cases of CPB. Clinical trials of this study, however, could not clarify the relationship between blood viscosity during CPB and postoperative neurologic complications, including impaired consciousness, seizures, cognitive impairment, and stroke. To this end, this method should be used for various cases, including deep hypothermia circulatory arrest procedures, and a large sample size should be investigated.

Because blood viscosity in the oxygenator is derived only from blood flow and pressure gradient, it was difficult to distinguish if the predicted increase in viscosity was a result of biofouling that narrowed the passage. Therefore, in a future study, the author plans to propose a solution to this problem by integrating this system by using an estimated blood viscosity algorithm that does not depend on the oxygenator. In previous studies, the direct effects of blood temperature and hematocrit on viscosity were reported [33]. Eckmann *et al.* developed a parametric expression for predicting blood viscosity based on variables that predicted the independent effects of temperature, shear rate, hematocrit, and diluent on blood viscosity [36]. In chapter 3, the effect of temperature change on viscosity was systematically investigated in bovine blood samples for three different hematocrit levels. For hematocrit levels of 20–40%, the relationship between temperature and viscosity fitted a linear approximation. Therefore, from this relationship, we are planning to propose the possibility that the viscosity (η_0) of the normal condition can be estimated with the following equation (Eq. 5.1):

$$\eta_0(T, Ht) = AT + B$$

$$A = -0.002Ht + 0.00339 \quad B = 0.1871Ht - 1.6264.$$

(5.1)

The above equation approximates η_0 from temperature (T) and hematocrit (Ht), where the included coefficients of the equations were obtained using a nonlinear least-squares method based on an expression relating T , Ht , and η even though these coefficient values were derived from bovine blood. Please note that the derivation of these coefficients for human blood requires the collection and analysis of relevant clinical data using this system in the future. Comparing η_0 calculated by T and Ht with η_e calculated by ΔP and Q may enable monitoring of the blockage of the oxygenator flow path because $\eta_0 \ll \eta_e$ indicates possible biofouling, which narrows the passage. This proposed method must demonstrate efficacy with oxygenator models such as coagulation and echinocyte.

Furthermore, a future study will also adapt this algorithm to other extracorporeal circulation (ECC) systems such as hemodialysis and continuous renal replacement therapy. Although these ECC systems do not use an oxygenator, this algorithm may estimate viscosity based on the pressure-flow characteristics of the hemofilter. This new algorithm for estimating viscosity should be useful for detecting various viscosity-related effects that may occur during ECC.

Publications concerning this dissertation are listed in the bibliography [46]–[50].

Bibliography

- [1] J. H. Gibbon Jr, "Application of a mechanical heart and lung apparatus to cardiac surgery," *Minn Med.*, vol. 37, no. 3, pp. 171-185, Mar. 1954.
- [2] K. Karkouti, W. S. Beattie, D. N. Wijeyesundera, V. Rao, C. Chan, K. M. Dattilo, G. Djiani, J. Ivanov, J. Karski, T. E. David, "Hemodilution during cardiopulmonary bypass is an independent risk factor for acute renal failure in adult cardiac surgery," *J. Thorac. Cardiovasc. Surg.*, vol. 129, no. 2, pp. 391-400, Feb. 2005.
- [3] M. Ranucci, B. De Toffol, G. Isgrò, F. Romitti, D. Conti, M. Vicentini, "Hyperlactatemia during cardiopulmonary bypass: determinants and impact on postoperative outcome," *Crit. Care.*, vol. 10, no. 6, Nov. 2006. DOI: 10.1186/cc5113.
- [4] R. F. Hickey, P. F. Hoar, "Whole-body oxygen consumption during low-flow hypothermic cardiopulmonary bypass," *J. Thorac. Cardiovasc. Surg.*, vol. 83, no. 6, pp. 903-906, 1983.
- [5] M. V. Kameneva, A. Ündar, J. F. Antaki, M. J. Watach, J. H. Calhoon, H. S. Borovetz, "Decrease in red blood cell deformability caused by hypothermia, hemodilution, and mechanical stress: factors related to cardiopulmonary bypass," *ASAIO J.*, vol. 45, no. 4, pp. 307-310, 1999.
- [6] T. Shiga, N. Maeda, K. Kon, "Erythrocyte rheology," *Crit. Rev. Oncol. Hematol.*, vol. 10, no. 1, pp. 9-48, 1990.
- [7] N. Maeda, "Erythrocyte rheology in microcirculation," *Jpn. J. Physiol.*, vol. 46, no. 1, pp. 1-14, Feb. 1996.

- [8] G. B. Thurston, N. M. Henderson, "Effects of flow geometry on blood viscoelasticity," *Biorheology*, vol. 43, no. 6, pp. 729-746, 2006.
- [9] A. Ündar, N. Henderson, G. B. Thurston, T. Masai, E. A. Beyer, O. H. Frazier, C. D. Fraser, Jr., "The effects of pulsatile versus nonpulsatile perfusion on blood viscoelasticity before and after deep hypothermic circulatory arrest in a neonatal piglet model," *Artificial Organs*, vol. 23, no. 8, pp. 717-721, Aug. 1999.
- [10] C. W. Hogue, Jr, C. A. Palin, J.E. Arrowsmith, D. Bainton, "Cardiopulmonary bypass management and neurologic outcomes: an evidence-based appraisal of current practices," *Anesth Analg*, vol. 103, no. 1, pp. 21-37, Jul. 2006.
- [11] R. E. Holsworth, Jr., L. M. Shecterle, J. A. St. Cyr, G. D. Sloop, "Importance of monitoring blood viscosity during cardiopulmonary bypass," *Perfusion*, vol. 28, no. 1, pp. 91-92, Jan. 2013.
- [12] D.J. Cook, W.C. Oliver, Jr, T. A. Orszulak, R.C. Daly, R. D. Bryce, "Cardiopulmonary bypass temperature, hematocrit, and cerebral oxygen delivery in humans," *Ann Thorac Surg*, vol. 60, no. 6, pp. 1671-1677, Dec. 1995.
- [13] P. Gaehtgens, P. Marx, "Hemorheological Aspects of the Pathophysiology of Cerebral Ischemia," *J Cereb Blood Flow Metab*, vol. 7, no. 3, pp. 259-265, Jun. 1987.
- [14] J. H. Wood, D. B. Kee, Jr, "Hemorheology of the cerebral circulation in stroke," *Stroke*, vol. 16, no. 5, pp. 765-772, Oct. 1985.
- [15] J. J. Jagers, M. C. Neal, P. K. Smith, R. M. Ungerleider, J. H. Lawson, "Infant cardiopulmonary bypass: a procoagulant state," *Ann Thorac Surg*, vol. 68, no. 2, pp. 513-520, Aug. 1999.

- [16] T. Tsuji, Y. Kashima, K. Muneoka, H. Kusano, T. Togawa, "Continuous tube viscometry of blood by a polypropylene hollow fiber oxygenator," *Tokyo Ika Shika Daigaku Iyo Kizai Kenkyusho Hokoku*, vol. 18, pp. 67-74, 1984. (In Japanese)
- [17] F. De Somer, "Does contemporary oxygenator design influence haemolysis?" *Perfusion*, vol. 28, no. 4, pp. 280-285, July 2013.
- [18] P. A. Drinker, R. H. Bartlett, R. M. Bialer, B. S. Noyes, Jr., "Augmentation of membrane gas transfer by induced secondary flows," *Surgery*, vol. 66, no. 4, pp. 775-781, Oct. 1969.
- [19] S. R. Wickramasinghe, C. M. Kahr, B. Han, "Mass transfer in blood oxygenators using blood analogue fluids," *Biotechnol. Prog.*, vol. 18, no. 4, pp. 867-873, July-Aug. 2002.
- [20] A. Nakamura, "Development of real-time blood viscometry during cardiopulmonary bypass," *Jpn J Extra-Corporeal Technology*, vol. 41, no. 2, pp. 123-130, 2013. (In Japanese)
- [21] A. R. Fisher, M. Baker, M. Buffin, P. Campbell, S. Hansbro, S. Kennington, A. Lilley, M. Whitehorne, "Normal and abnormal trans-oxygenator pressure gradients during cardiopulmonary bypass," *Perfusion*, vol. 18, no. 1, pp. 25-30, Mar. 2003.
- [22] M. Ranucci, T. Laddomada, M. Ranucci, E. Baryshnikova, "Blood viscosity during coagulation at different shear rates," *Physiol. Rep.*, vol. 2, no. 7, July 2014. DOI: 10.14814/phy2.12065.

- [23] J. W. Hoffman, Jr., T. B. Gilbert, M. L. Hyder, "Cold agglutinins complicating repair of aortic dissection using cardiopulmonary bypass and hypothermic circulatory arrest: case report and review," *Perfusion*, vol. 17, pp. 391-394, Sept. 2002.
- [24] W. H. Reinhart, S. Chien, "Red cell rheology in stomatocyte echinocyte transformation: roles of cell geometry and cell shape," *Blood*, vol. 67, no. 4, pp. 1110-1118, Apr. 1986.
- [25] N. Okamura, A. Tokumine, M. Otsuki, S. Okahara, T. Kurosaki, S. Ninomiya, "Basic study on fluid mechanics characteristics of artificial lung," *Jpn J Extra-Corporeal Technology*, vol. 37, no. 3, pp. 347-350, Sep. 2010. (In Japanese)
- [26] A. S. Popel, P. C. Johnson, "Microcirculation and hemorheology," *Annu Rev Fluid Mech*, vol. 37, no. 1, pp. 43-69, Jan. 2005.
- [27] D. A. Fedosov, B. Caswell, A. S. Popel, G. E. Karniadakis, "Blood flow and cell-free layer in microvessels," *Microcirculation*, vol. 17, no. 8, pp. 615-628, Nov. 2010.
- [28] A. R. Pries, D. Neuhaus, P. Gaehtgens, "Blood viscosity in tube flow: dependence on diameter and hematocrit," *Am J Physiol*, vol. 263, no.6, pp. 1770-1778, Dec. 1992.
- [29] R. L. Whitmore, "The flow behaviour of blood in the circulation," *Nature*, vol. 215, no. 5097, pp. 123-126, Jul. 1967.
- [30] E. W. Merrill, E. R. Gilliland, G. Cokelet, H. Shin, A. Britten, R. E. Wells Jr, "Rheology of human blood, near and at zero flow. Effects of temperature and hematocrit level," *Biophys J*, vol. 3, pp. 199-213, May. 1963.

- [31] V. Travagli, I. Zanardi, L. Boschi, A. Gabbrielli, A. Vita, M. Mastronuzzi, R. Cappelli, S. Forconi, "Comparison of blood viscosity using a torsional oscillation viscometer and a rheometer," *Clin. Hemorheol. Microcirc.*, vol. 38, no. 2, pp. 65-74, 2008.
- [32] Y. Ganushchak, W. van Marken Lichtenbelt, T. van der Nagel, D. S. de Jong, "Hydrodynamic performance and heat generation by centrifugal pumps," *Perfusion*, vol. 21, no. 6, pp. 373-379, Nov. 2006.
- [33] P. W. Rand, E. Lacombe, HE. Hunt, WH. Austin, "Viscosity of normal human blood under normothermic and hypothermic conditions," *J Appl Physiol*, vol. 19, pp. 117-122, Jan. 1964.
- [34] M. London, "The role of blood rheology in regulating blood pressure.," *Clin Hemorheol Microcirc*, vol. 17, no. 2, pp. 93-106, Mar-Apr. 1997.
- [35] S. Smale, "On the efficiency algorithms of analysis," *Bull. Amer. Math. Soc*, vol. 13. No. 2, pp. 87-121, Oct. 1985.
- [36] D. M. Eckmann, S. Bowers, M. Stecker, A. T. Cheung, "Hematocrit, volume expander, temperature, and shear rate effects on blood viscosity," *Anesth. Analg.*, vol. 91, no. 3, pp. 539-545, Sept. 2000.
- [37] V. Travagli, I. Zanardi, L. Boschi, V. Turchetti, S. Forconi, "Evaluation of a torsional-vibrating technique for the hemorheological characterization," *Clinical Hemorheology and Microcirculation*, vol. 35, no. 1-2, pp. 283-289, 2006.
- [38] K Gester, SV Jansen, M Stahl, U Steinseifer, "A simple method for the investigation of cell separation effects of blood with physiological hematocrit values," *Artificial Organs*, vol. 39, no. 5, pp. 432-440, May. 2015.

- [39] T. M. Amin, J. A. Sirs, "The blood rheology of man and various animal species," *Q J Exp Physio*, vol. 70, no. 1, pp. 37-49, Jan. 1985.
- [40] R. F. Davis, M. Kurusz, V. R. Conti. "Circuitry and cannulation techniques, in *Cardiopulmonary Bypass: Principles and Practice*, 3rd ed., G. P. Gravlee, R. F. Davis, A. H. Stammers, R. M. Ungerleider, Eds. Philadelphia, PA: Lippincott Williams & Wilkins, 2008, pp. 543-571.
- [41] L. Rigg, B. Searles, E. M. Darling, "A 2013 survey on pressure monitoring in adult cardiopulmonary bypass circuits: modes and applications," *J. Extra Corpor. Technol.*, vol. 46, no. 4, pp. 287-292, Dec. 2014.
- [42] D. M. Nasr, A. A. Rabinstein, "Neurologic complications of extracorporeal membrane oxygenation," *J. Clin. Neurol.*, vol. 11, no. 4, pp. 383-389, Oct. 2015.
- [43] Y. Niimi, F. Ichinose, Y. Ishiguro, K. Terui, S. Uezono, S. Morita, S. Yamane, "The effects of heparin coating of oxygenator fibers on platelet adhesion and protein adsorption," *Anesth. Analg.*, vol. 89, no. 3, pp. 573-579, Sept. 1999.
- [44] F. Qiu, S. Peng, A. Kunselman, A. Ündar, "Evaluation of Capiox FX05 Oxygenator with an integrated arterial filter on trapping gaseous microemboli and pressure drop with open and closed purge line," *Artificial Organs*, vol. 34, no. 11, pp. 1053-1057, Nov. 2010.
- [45] J. W. Yarnell, I. A. Baker, P. M. Sweetnam, D. Bainton, J. R. O'Brien, P. J. Whitehead, P. C. Elwood, "Fibrinogen, viscosity, and white blood cell count are major risk factors for ischemic heart disease: The Caerphilly and Speedwell collaborative heart disease studies," *Circulation*, vol. 83, no. 3, pp. 836-844, Mar. 1991.

- [46] S. Okahara, T. Tsuji, S. Ninomiya, S. Miyamoto, H. Takahashi, Z. Soh, T. Sueda, “Hydrodynamic characteristics of a membrane oxygenator: modeling of pressure-flow characteristics and their influence on apparent viscosity,” *Perfusion*, vol. 30, no. 6, pp. 478-483, Sept. 2015.
- [47] S. Okahara, T. Tsuji, Z. Soh, T. Sueda, “A blood viscosity estimation method based on pressure-flow characteristics of an oxygenator during cardiopulmonary bypass and its clinical application,” *Conf. Proc. IEEE Eng. Med. Biol. Soc.*, Milan, Italy, 2015, pp. 5525-5528.
- [48] S. Okahara, Z. Soh, S. Miyamoto, H. Takahashi, H. Itoh, S. Takahashi, T. Sueda, T. Tsuji, “A novel blood viscosity estimation method based on pressure-flow characteristics of an oxygenator during cardiopulmonary bypass,” *Artificial Organs*, 2016. (in press)
- [49] S. Okahara, Z. Soh, S. Takahashi, T. Sueda, T. Tsuji, “Blood viscosity monitoring during cardiopulmonary bypass based on pressure-flow characteristics of a Newtonian fluid,” *Conf. Proc. IEEE Eng. Med. Biol. Soc.*, Orlando, FL, USA, 2015, pp. 2331-2334.
- [50] S. Okahara, Z. Soh, S. Miyamoto, H. Takahashi, S. Takahashi, T. Sueda, T. Tsuji, “Continuous blood viscosity monitoring system for cardiopulmonary bypass applications,” *IEEE Transactions on Biomedical Engineering*, 2016. (in press)

Acknowledgments

I would like to express my deepest gratitude to my supervisor, Professor Toshio Tsuji, for his elaborate guidance, considerable encouragement and invaluable discussion that made my research a great achievement and my study life unforgettable. His perpetual energy and enthusiasm in research extremely motivated me in my studies.

I am also grateful to committee members Professor Idaku Ishii and Professor Toru Yamamoto for their invaluable suggestions and opinions on this dissertation.

I especially would like to express my sincere appreciation to my adviser, Dr. Zu Soh, for his advice, suggestions, encouragement and patience. His scientific expertise helped me immensely in many aspects from planning the studies to the final revision of the papers.

I am very grateful to Professor Taijiro Sueda, Dr. Shinya Takahashi, Mr. Hidenobu Takahashi, and Mr. Satoshi Miyamoto for their valuable cooperation in clinical experiments at Hiroshima University Hospital.

My thanks also go to Professor Hideshi Itoh at Junshin Gakuen University, for your kind efforts to support my research, my spirit and my daily life.

Finally, I am forever indebted to my family for their endless love, understanding, support, encouragement and sacrifice throughout my studies.

This work was partially supported by Japan Society for the Promotion of Science (JSPS) KAKENHI Grant Number 16K01429.